FACULDADE DE ENGENHARIA DA UNIVERSIDADE DO PORTO

Software Defined Radar for Medical Imaging

Wilson José dos Santos Silva

Integrated Master in Electrical and Computers Engineering

Supervisor: João Paulo Trigueiros da Silva Cunha (FEUP/INESC TEC)

Co-Supervisor: Luís Manuel de Sousa Pessoa (INESC TEC)

July 18, 2016

Resumo

Tal como Maslow reconheceu na sua hierarquia das necessidades, a saúde é o sustentáculo do sentimento de completude e o que permite ao ser humano atingir todo o seu potencial. Na impossibilidade de impedir a ocorrência de uma doença, o nosso foco deve estar na sua rápida e eficiente deteção.

Reconhecendo a importância da saúde, diversos investigadores dedicaram a sua vida na tentativa de maximizar o sucesso do diagnóstico. Contudo, os sistemas que existem atualmente não são perfeitos. Alguns deles são caros, outros não possuem a resolução necessária e outros ainda são demasiado pesados para serem portáveis.

Nos últimos anos, sistemas de imagem baseados em micro-ondas emergiram como uma ferramenta importante na deteção de uma doença devido às suas propriedades não-ionizantes e não invasivas, ao seu potencial de baixo-custo e ao facto de possuírem uma resolução adequada.

Para além desta aplicação, estes sistemas têm sido também usados na monitorização de sinais vitais e tumores.

Neste trabalho é analisada a literatura de *Microwave Human Bio-sensing* e *Microwave Medical Imaging*. Adicionalmente, são propostos dois sistemas inovadores baseados na tecnologia *Software Defined Radar*.

O primeiro sistema é capaz de detetar interrupções no ciclo respiratório e calcular eficazmente a sua frequência. Além do mais, este facilmente incorpora novas capacidades, tais como cálculo de frequência cardíaca e localização de pessoas ou objetos. O facto deste sistema ter como base o uso de micro-ondas permite a não utilização de sensores em contacto com o corpo humano e, consequentemente, evita desconforto e irritação da pele. Adequa-se, portanto, a aplicações típicas, como detecção de apneia do sono e monitorização de crianças, ou a aplicações emergentes como o controlo de sinais vitais em condutores de automóveis.

Por sua vez, o segundo sistema é capaz de detetar a presença de materiais com diferentes propriedades dielétricas dentro de um fantoma. Tal característica pode ser explorada em certos cenários, como por exemplo, na identificação do tipo de AVC, no diagnóstico de cancro mamário e na deteção de ataques cardíacos. Sistemas de micro-ondas baseados no uso de *Vector Network Analyzers* (VNAs) demonstraram ser bem sucedidos na identificação do tipo de AVC (isquémico ou hemorrágico). Ao usarmos um *Software Defined Radio* em substituição do VNA, a portabilidade do sistema final é aumentada e o seu custo diminuido. Ambas as consequências podem ser fundamentais para tornar o tratamento trombolítico possível em ambiente pré-hospitalar, o que levaria a uma diminuição ou mesmo eliminação de danos permanentes em pacientes com AVCs insquémicos.

Em suma, consideramos que este trabalho demonstra o potencial disruptivo da tecnologia *Software Defined Radar*. Quando comparado com dispositivos convencionais, esta tecnologia introduz diversas características vantajosas, tais como, a possibilidade de múltiplas aplicações, capacidade de realizar processamentos complexos, portabilidade e baixo-custo.

Abstract

As Maslow has recognized in his hierarchy of needs, health is the basis for fulfillment and higher achievements. Since it is impossible not to suffer from diseases, our focus should be on detecting them as soon as possible and with high certainty.

Recognizing health's importance, several researchers have dedicated their lives in order to maximize the success of a diagnosis. However, the existing systems are not perfect. Some of them are expensive, others suffer from lack of sensitivity and others are too heavy to be portable.

In the last years, Microwave Imaging emerged as an important tool for recognizing a disease due to its non-invasive and non-ionizing nature, low-cost potential and efficient resolution.

Microwaves have also been used in cardiopulmonary sensing or tumor tracking, making a constant monitoring of vital signs possible.

In this work, we analyze the state-of-the-art in Microwave Human Bio-sensing and Microwave Medical Imaging. Moreover, we present two different and novel system prototypes based on Software Defined Radar technology.

The first prototype is able to detect interruptions in the normal breathing motion and computes effectively the respiration frequency. Furthermore, it can easily incorporate additional capabilities such as heart rate calculation or subject's localization. Since it works using microwaves, it does not require any sensor attached to the body and consequently does not cause discomfort nor skin irritation. It is thus well suited for traditional applications such as sleep apnea detection and infant observation or emerging applications as the automobile market.

Our second prototype is capable of detecting the presence of different dielectric materials inside a phantom. That characteristic can be exploited in certain scenarios such as stroke identification, breast cancer diagnosis and heart failure detection. Microwave systems consisting on Vector Network Analyzers (VNAs) have proved to be successful in identifying stroke's type (ischemic or hemorrhagic). As we are using a Software Defined Radio instead of the commonly used VNA, portability is increased and cost is reduced. Those consequences are fundamental for prehospital thrombolytic treatment to be possible, which could lead to a reduction or even abolishment of permanent damage in ischemic patients.

Overall, we feel that this work has demonstrated the disruptive potential of Software Defined Radar technology. Compared to the traditional devices, it introduces many advantageous features such as multipurpose, portability, low-cost and complex processing capabilities.

Acknowledgements

First of all I would like to thank my supervisor, João Paulo Cunha, for the idea of this dissertation and for his guidance during this work. I would also like to thank my co-supervisor, Luís Pessoa, for his valuable insights.

Moreover, I want to thank all my friends for their support and enthusiasm. I feel that I would be a lot worse if I haven't met you.

Furthermore, I would like to express my gratitude to my family for supporting me during my entire life and especially in the most difficult situations.

I also want to thank my girlfriend, Patrícia, for loving me. I couldn't ask for more.

Finally, I would like to dedicate this dissertation to my grandfather, Mário da Silva, for showing me that someone is never too old or too sick to achieve something.

Wilson Silva

"On the mountains of truth you will never climb in vain: either you will get up higher today, or you will exercise your strength so as to be able to get up higher tomorrow."

Friedrich Nietzsche

Contents

List of Figures

List of Tables

Abbreviations

ADC	Analog-to-Digital Converter
BB	Base-band
BPF	Bandpass Filter
CMOS	Complementary Metal-Oxide-Semiconductor
CT	Computer Tomography
CW	Continuous-Wave
DAC	Digital-to-Analog Converter
DAS	Delay and Sum
EIRP	Equivalent Isotropically Radiated Power
FCC	Federal Communications Commission
FPGA	Field Programmable Gate Array
ICA	Independet Component Analysis
IF	Intermediate Frequency
LO	Local Oscillator
MRI	Magnetic Resonance Imaging
MWI	Microwave Imaging
RADAR	Radio Detection and Ranging
RF	Radio Frequency
Rx	Receive
SD	Subspace Distance
SIDS	Sudden Infant Death Syndrome
SDR	Software Defined Radio
SDRadar	Software Defined Radar
SFCW	Stepped Frequency Continuous Wave
TEM	Transverse Electromagnetic
Tx	Transmit
UAV	Unmanned Aerial Vehicles
USRP	Universal Software Radio Peripheral
UWB	Ultra Wideband
VNA	Vector Network Analyzer

Chapter 1

Introduction

1.1 Motivation

In many clinical situations, the quality of a medical diagnosis is highly dependent on the technology which is available to the doctor at that time. There are several different technologies used in this field, particularly Medical Imaging modalities such as X-Ray, Ultrasound, Computed Tomography and Magnetic Resonance. All of them have relevant drawbacks.

Ultrasound imaging is a cost effective technology. However, it has limited sensitivity and requires bulky instruments [1]. Magnetic Resonance Imaging and Computed Tomography, on the other hand, offer high resolution at the expense of high cost and heavy machinery. X-Ray is between the four the most widely used due to its high resolution and affordable price [2].

Apart from cost and resolution, it is important to analyse the effects of the technologies on the human tissues. One of the X-Ray's weaknesses is related to that. It causes ionization which can be harmful to human health [3].

Microwave Imaging (MWI) arises as a possible solution to overcome the previous problems. It is a non-invasive and non-ionizing technique which only requires a low amount of power to work conveniently. Moreover, when compared to the alternatives, its cost is very reasonable. Depending on frequency range, MWI can be very cheap.

MWI consists on the transmission of a microwave signal and consequent measuring of the characteristics of the backscattered signal, in other words, a Radar. In the Medical field, it is well-suited for the detection of breast cancer, brain stroke and heart failure, which are major causes of death.

Breast cancer is the most common type of cancer affecting female population. An early stage detection is of extreme importance and this can be achieved using microwave imaging. It allows a cost effective, more comfortable examination than X-Ray mammography which can be painful due to the compression of the breast. The existing contrast between the dielectric properties of healthy and cancerous tissues enables the detection.

Stroke is responsible, worldwide, for millions of deaths each year and it is the leading cause of neurological dysfunction. There are two types of strokes: ischemic (blood clot induced) and

hemorrhagic (bleeding) strokes. Both have similar symptoms but the medical treatments that they require are completely different. Usually, a CT (Computed Tomography) is used but a Radar scanning the brain can also determine if there is bleeding or not, in other words, if the stroke is hemorrhagic or ischemic. This is achieved by processing adequately the backscattered signals.

In recent years, heart failure became a serious problem due to the actual way of living. Since there is an association between the amount of fluids in lungs and heart failure, it is also possible to use MWI to detect the occurrence.

1.2 Objectives

In the previous section, the reasons for using Microwave Imaging for Medical applications were presented. The literature shows the feasibility of implementing this technique using a Vector Network Analyzer (VNA) as an adequate transceiver for the purpose. The VNA is capable of synthetically generate ultra-wideband (UWB) pulses by transmitting a set of narrowband stepped frequency continuous waveforms (SFCW) over a wide range of frequencies, while receiving the respective backscattered signals from the human tissue [4]. However, the VNA is an expensive and heavy device. The goal of this dissertation is to replace the VNA for a Software Defined Radio (SDR), which is portable and low-cost. Furthermore and making use of the large capabilities of SDR technology, a system capable of monitoring vital signs will also be created.

A Software Defined Radar, which is nothing more than a Software Defined Radio with radar purposes, is constituted by a computer, a reconfigurable integrated circuit, filters, amplifiers and antennas. On the computer side, GNU Radio [5] will be used to define the transmitted waveforms and to process the received data. Regarding the hardware platform, we will use USRP B200 [6], which already includes the filters and amplifiers needed. To complete our system, Horn and Log Periodic PCB antennas will be added.

1.3 Contributions

The main contribution of this dissertation was the demonstration of the large potential of Software-Defined Radar technology in the health domain.

Concerning Human Bio-sensing, we have developed a novel and reconfigurable platform, which is capable of monitoring human respiration, providing contactless respiration rate measurements for different scenarios such as the automobile market. Furthermore, it can easily incorporate additional capabilities such as heart rate calculation or subject's localization.

Regarding Microwave Medical Imaging, we have shown that it is possible to replace the expensive materials currently used for low-cost equipment. A new reconfigurable system capable of specifying frequency of operation in real-time was developed. It was designed in order to be more portable and low-cost than the actual systems. With those characteristics, prehospital thrombolytic treatment could be possible and a reduction or even abolishment of permanent damage in ischemic patients would be achieved.

1.4 Organization

In addition to the Introduction, this document contains six more chapters. Chapter 2 demonstrates the different existent modalities used to monitor vital signs. In Chapter 3, the state of the art in Microwave Medical Imaging is given, showing different applications and different approaches already made in each application. An analysis of the hardware and software platforms available on the market is done in Chapter 4. Chapter 5 and Chapter 6 explain in detail the system implementation and the results achieved in Human Bio-Sensing and Medical Imaging, respectively. Finally, in Chapter 7, we discuss our work and propose future tasks to be done.

Chapter 2

Microwave Human Bio-sensing

This section illustrates the use of a radar in order to measure some human vital signs, namely, heartbeat and respiration.

2.1 Continuous Wave Doppler Radar

2.1.1 Introduction

A Doppler Radar can be considered as the simplest configuration possible of a Radar. Its principle is based on detecting a frequency or phase shift in the received backscattered signal. That characteristic makes it well suited for the measurement of both breathing and heartbeat, without the need of any sensor attached to the body [7].

The use of Microwave Doppler Radar for detection of physiological movements have started in the early 1970s [8]. Since then it was already demonstrated that it is a successful method. Nowadays, most of the research is done on its technological improvement, in order to achieve better accuracy, power consumption, longer detection range and smaller form factor [7].

Being a non-contact measurement method, Microwave Doppler Radar has numerous advantages when compared to traditional monitoring methods. Unlike conventional methods, which require electrodes or straps, it does not cause discomfort nor skin irritation [9]. That is especially important when it is necessary a long-term continuous monitoring and when the patients have severe burns [10]. Since usually people do not like to be connected to measuring devices nor to be aware of constant monitoring [11], microwave sensing is a much more "friendly" sensing technique.

Its applications are diverse and of great importance, including outpatient care, patient monitoring, physical therapy, elderly care [12], sports/fitness training, long-term monitoring of chronic health conditions [13], survivor detection in search and rescue operations [14], through-wall detection for military and security operations [15], sleep apnea detection [16] and monitoring and infant observation [17].

One of the major causes of infant mortality (third leading cause) is Sudden Infant Death Syndrome (SIDS) [18], [9]. A Doppler Radar enables the detection of tiny baby movements induced

by breathing. If the baby stops breathing and consequently stops moving, the system detects this event and depending on the time span without movement can send an alert to the baby's parents.

Sleep Apnea/Hypoapnea Syndrome (SAHS) is characterized by repetitive punctuations or reductions of respiration during sleep. It is estimated that circa 4% of middle-aged man suffer from that disease [16]. The gold standard for a definitive diagnosis of the SAHS is polysomnography, which involves an overnight multi-channel recording in a specialized sleep laboratory. Polysomnography is an expensive and time-consuming procedure, with extensive resources invested in patients with mild or moderate disease. Since SAHS elicits a unique heart rate rhythm of brady-tachycardia [16], a system monitoring heart rate as one using CW Radar is capable of detecting that disease.

The ratio of those aged 65 and older is extremely high nowadays, especially in Japan, which has the world's fastest aging society. In order to monitor the health of the elderly, devices will be needed that can easily monitor vital signs at home or in hospitals and nursing facilities. Circulatory and respiratory issues in particular pose a risk for the elderly, because they can lead to potentially serious conditions. Therefore, monitoring cardiac and respiratory functions is important. However, long-term monitoring using electrodes places a heavy burden on monitored individuals. Bedsores are common in bedridden elderly persons, and in these cases it is difficult to place electrodes on the skin. For this reason, it is necessary to develop non-contact and unconstrained vital sign measurement methods [10].

Additionally, emerging applications for short-range vital sign monitoring are showing up, for example [19]:

1) Automotive safety systems: Here, there is an interest to detect the heart rate of drivers in order to detect erratic heart rate which can be caused by use of drugs and lack of sleep

2) Kiosks and Automatic Teller Machines - In security checkpoints, airport ticket kiosks, and bank teller machines there is an interest in screening erratic heart activity as well

3) Airports/Casinos - Finally, in airports and casinos, it is of great interest monitoring heart activity in order to detecting unusual physiological activity characteristic of someone who is hiding something

2.1.2 Measurement and Processing

The vital sign detection is achieved sending an unmodulated signal (2.1) towards the human body and then analyzing the resultant phase shift of the backscattered signal (2.2) [20].

$$T(t) = cos[2\pi ft + \phi(t)] \tag{2.1}$$

$$R(t) \approx cos[2\pi ft - \frac{4\pi d_o}{\lambda} - \frac{4\pi x(t)}{\lambda} + \pi(t - \frac{2d_o}{c})] \tag{2.2}$$

In (2.2), d_o represents the nominal distance at which the human body is from the radar and x(t) is the physiological movement. As can be easily seen, the received signal is similar to the

transmitted one but suffers from a time delay, determined by the nominal distance, and a phase shift, due to the periodic motion of the target.

In order to process the signal, a down-conversion is recommended and possible using as Local Oscillator (LO) the same transmitted signal, resulting in the following signal (where θ is determined by the nominal detection distance):

$$B(t) = cos[\theta - \frac{4\pi x(t)}{\lambda} + \Delta\phi(t)] \tag{2.3}$$

Since our object of interest is the human chest, the demodulated signal is then proportional to the periodic displacement due to respiration and heart beat [20].

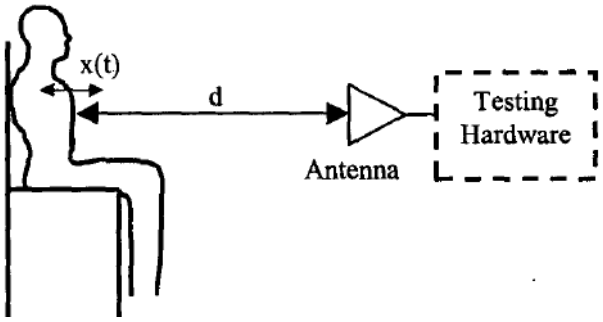

Figure 2.1: Testing Setup. Taken from [20]

The chest movement is mainly caused by respiration, which is characterized by typical frequencies between 0.1 Hz and 0.8 Hz. Heartbeat frequency is usually higher (0.8 Hz - 2 Hz) [17].

To achieve monitoring vital signs, a wide range of transmitted frequencies was used in the past (1 GHz to 35 GHz [21]). The most suitable frequency of operation depends on the distance of measurement and penetration requirements. For example, in activities of search and rescue when it is necessary for the beam to penetrate earthquake rubble or collapsed building debris, low frequencies are more suitable (e.g. 1.150 GHz).

2.1.3 Separation of Heartbeat and Respiration

One of the biggest challenges when sensing vital signs is how to find the part of the backscattered signal caused by heartbeat alone. That is due to the fact that the respiratory signal is much stronger (10 to 100 times) than the signal from the heart [12]. Band-pass filtering of the resulting signal might not remove all the respiratory components since even if the fundamental frequency of respiration is lower, harmonics might fall into the same frequency spectrum as heartbeat signal.

To effectively isolate the desired heart beat signal one can use Blind Source Separation algorithms [22], which consist on the separation of a source signal from mixed signals, without relevant information about them. One of the most famous algorithms following those rules is Independent Component Analysis (ICA). ICA is a statistical and computational technique for revealing hidden factors that underlie sets of random variables, measurements or signals [23]. [22]

and [12] show the feasibility of ICA on the separation of respiration and heartbeat signals. However, there are other algorithms being tested as is shown in [24].

2.2 UWB Radar

Ultra-Wideband Radar is also a solution for noncontact Human Bio-sensing. It has advantages and disadvantages when compared to CW Doppler Radar. The CW Doppler Radar is better in terms of complexity and power consumption. UWB is better because it allows the elimination of interference caused by multi-path reflection.

A signal is categorized as UWB signal if its bandwidth is very large with respect to its center frequency [25]. The advantages of wideband signals with respect to narrowband signals are the following:

1. Fine time resolution enabled by large instantaneous bandwidth

2. Short duration pulses that provide robust performance in dense multipath environments by exploiting more resolvable paths

3. Low power spectral density that allows coexistence with existing users and has low probability of intercept

4. Data rate may be traded for power spectral density and multipath performance

As a pulse radar, UWB range resolution of target detection is given by (2.4).

$$\Delta d = \frac{c}{2 * BW} = \frac{\tau * c}{2} \tag{2.4}$$

In (2.4), c is the speed of electromagnetic wave, BW is the bandwidth of radar pulse in frequency domain and τ is the width of the radar pulse in time domain.

The pulses are emitted through an antenna. Then, when the signal encounters an object, there will be a reflected signal with a fraction of the energy sent. The computation of the distance is done based on the time delay between transmitted and received signal (2.5).

$$d = \frac{\Delta t * c}{2} \tag{2.5}$$

The use of UWB to monitor breathing is possible because the breathing motion causes periodic changes in the received signal at a distance where the target is located. The periodic change is reflected across multiple scans and the use of a reference scan allows to detect the motion. In [25], they have used moving average reference technique to achieve that goal and were successful. Apart from the typical respiration and heartbeat monitoring, UWB was also used on Aortic Pressure Estimation [26].

2.3 Discussion

As exposed in the foregoing sections, there are plenty of different applications for a Human Biosensing system, including infant observation, sleep apnea detection and elderly care.

The use of microwaves represents a major improvement over the rest of the systems currently used due to its contactless nature. Non-contact can be of extreme importance in cases of long-term monitoring or when patients have severe burns, as it is explained in this chapter.

Currently, each system is specifically designed for a determined application. In other words, hardware and software are designed to solve a particular problem and are useless in a little different scenario.

Then, it is of great interest to have a system, which is able to adapt to different scenarios. Moreover, this future system should also be capable of implementing advanced signal processing algorithms (as the ones used for separation of heartbeat and respiration).

Chapter 3

Microwave Medical Imaging

The importance of a correct diagnosis is enormous. A precise diagnosis made as soon as possible can improve the quality of life and even prevent a possible death. In order to develop a flawless, comfortable and low-cost diagnostic tool many academic research has been done. In the most recent years, Microwave Imaging arised as a major technology in diagnosis based on its non-ionizing nature, accurate results and low-cost potential.

It is possible to find its application in diseases such as:

- **Strokes**;
- **Breast Cancer**;
- **Heart Failures**;

In this chapter, a literature review of the application of Microwave Imaging in the referred diseases will be done, along with the characteristics of each system and its working principles.

3.1 Strokes

In Sweden 30 000 people suffer a stroke each year [27], in the United States the number is as high as 700 000 people and in Australia the number of people is 40 000 [28]. Those three examples illustrate the dimension of the problem, which is the second leading cause of death in the world [29].

There are two different types of brain sroke [28], ischemic and hemorrhagic. Ischemic strokes are caused by blood clots in the blood vessels, while hemorrhagic ones occur due to the bleeding within the area of brain or in the space surrounding. Approximately 85 % of all strokes are ischemic and just 15 % are bleeding strokes [30].

A treatment called thrombolysis is proved to be very successful for ischemic stroke patients when done in an early phase [30]. But, when given to hemorrhagic stroke patients, it can cause death. It is then, of extreme importance an early and precise diagnostic.

Principle of Detection

It is known that electromagnetic waves at microwave frequencies have the ability of penetrating the human body [31]. Taking advantage of that fact, it is possible to investigate the inner parts of the body searching for abnormalities. In this particular case, our interest is on detecting a stroke and identifying its type.

When a stroke occurs, independently of its type, it will change the dielectric properties of a particular region of the brain. In the hemorrhagic case, a pool of blood is caused, which has different dielectric characteristics than white and grey matter, enabling detection. The equivalent principle applies for ischemic strokes, since a blood clot obstructing a vessel prevents blood circulation and, consequently, oxygenation does not happen [32].

Frequency Dependence

Dielectric properties are not fixed values, they depend on frequency. The relation between the dielectric properties of the biological tissues and frequency is well defined by Deby's formula [33]:

$$\varepsilon_r(f) - \frac{\sigma(f)}{j2\pi f\varepsilon_o} = \varepsilon_\infty \sum_{i=1,2} \frac{\delta\varepsilon_i}{1+j2\pi f\tau_i} \tag{3.1}$$

Equation 3.1 is valid until frequencies up to 20 GHz [34] and the parameters are defined in [33], being ε_r the relative permittivity of the tissue and σ its conductivity. A helpful representation of the behaviour of those parameters with frequency is shown in Figures 3.1 and 3.2.

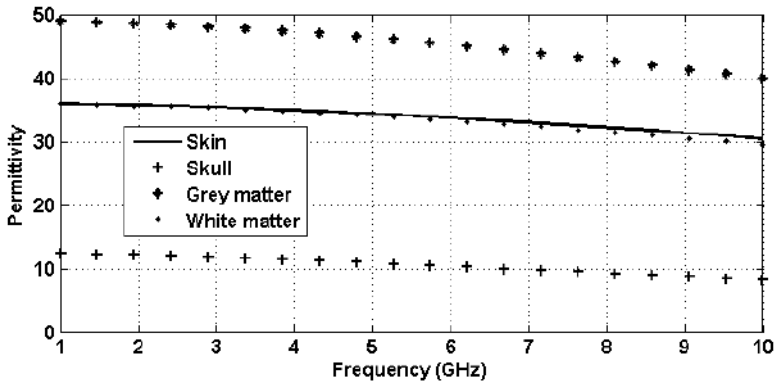

Figure 3.1: Relative Permittivity of different layers of the head considered vs. frequency. Taken from [34]

Another important aspect referred in [34] was the relation between attenuation and frequency. To obtain a graphical representation they have used:

$$\alpha(f) = \frac{2\pi f}{c_o}\sqrt{\frac{\varepsilon'}{2}\left(\sqrt{1+\left(\frac{\varepsilon''}{\varepsilon'}\right)^2}-1\right)} \tag{3.2}$$

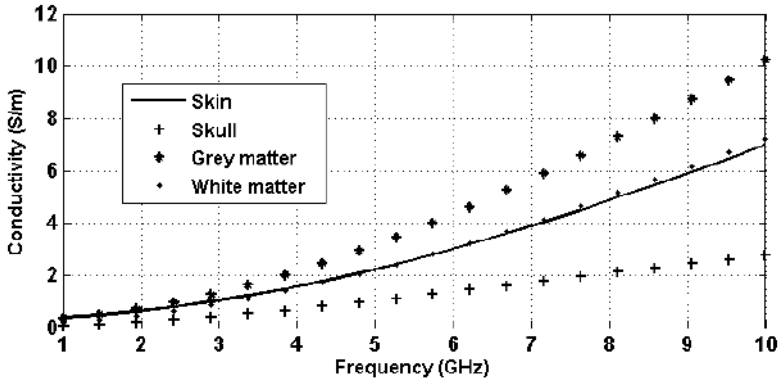

Figure 3.2: Conductivity of different layers of the head considered vs. frequency. Taken from [34]

where f is the operating frequency, c_o is the speed of light, ε' and ε" are the real and imaginary parts of the relative permittivity of the tissue at the operating frequency.

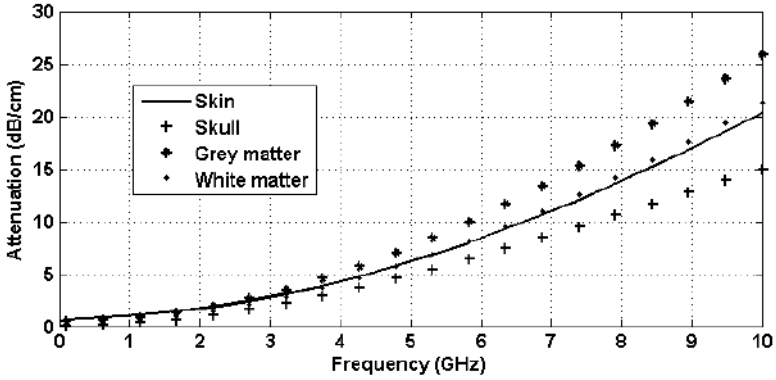

Figure 3.3: Attenuation per distance of the UWB signals in the different head layers vs. frequency. Taken from [34]

Although frequency enhances resolution, the suitable frequencies for stroke detection cannot be very high. That is clear in Figure 3.3. Since attenuation increases rapidly with an increase in frequency, it is a limiting factor of the resolution in microwave imaging.

Methodologies

There are several different implementations and experimental setups that can be found on literature. The principle consists always on sending electromagnetic waves and collecting the resultant backscattered signals for further processing and analysis. However, there is a diversity of antennas [35] and configurations used.

For instance, Fhager *et al* [30] developed a system based on the microwave tomography strategy. To transmit and receive the desired signals, they have used 10 triangular patch antennas, which were mounted inside a normal bicycle helmet (Figure 3.4) [36]. Doing that, the skull becomes surrounded by antennas. Every possible configuration of antennas as transmitter and

receiver is tried, so the consequent results, in terms of localization, are more reliable. A Vector Network Analyser is used to generate the transmitted signal and to collect the received signals, being both in the frequency range of 100 MHz to 3 GHz.

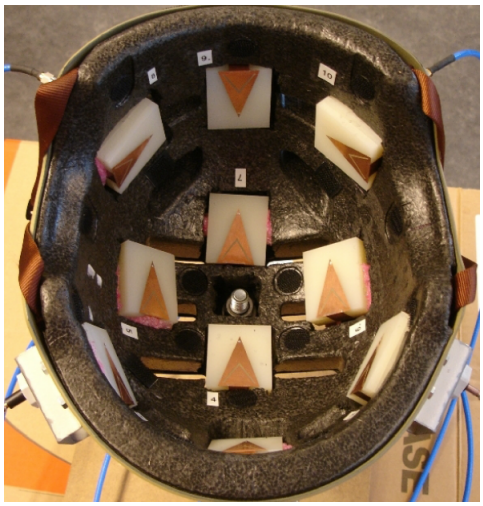

Figure 3.4: Antennas mounted inside a bicycle helmet. Taken from [30]

In order to achieve a functional system it is necessary to fill the gap of air between the antennas and the skull, since that would provoke reflections, which occur due to a mismatch in impedance (only when the impedances are the same the reflection coefficient is zero, equation 3.3). To overcome that problem, they have used plastic bags filled with a matching liquid, which were attached inside the helmet covering the antennas.

$$\Gamma = \frac{Z_L - Zo}{Z_L + Z_o} \tag{3.3}$$

In [37], they also take into account the necessity of the matching liquid, which they choose to be characterized by a permittivity similar to the average of the human head. Nonetheless, they used tapered-slot antennas and the frequency band 0.5-2 GHz.

[38] refers a system with the same goal but this one takes advantage of the synthetic aperture-based approach, which allows an improvement of resolution. Instead of 10 patch antennas, two moving travelling wave Vivaldi antennas are used. One of them transmits an UWB signal in the 1.5-5 GHz frequency range and the other receives the backscattered signals, in other words, it is used a bistatic configuration.

Object of Analysis

Ideally, experimental tests would be done in a person in a real-time situation. However, it is not possible to have a person having a stroke and available for experiments all the time. Therefore, phantoms [36] and computational models [34] [39] are usually used to verify the behaviour of the system.

Regarding computational models, the simulated head model can be considered as being composed of four different layers, namely, skin, skull, grey and white matter. Each of those layers

is characterized by a certain permittivity value, which will be different from the one of a stroke (Table 3.1 illustrates possible values).

Layer	Thickness/Radius (mm)	Permittivity
Skin	1/90	36
Skull	2/89	12
Grey Matter	22/87	48
White Matter	65/65	46
Stroke	30/15	60

Table 3.1: Frequency-dependent properties of tissues for a standard average person

On the other hand, if it is desired a more "physical" experience, a phantom can be used. Here, the idea is to use materials with determined permittivity values, in order to verify if the system meets its assumptions. We can decide to use a phantom that mimics brain properties or just use a random material because the most important aspect here is to have a difference in permittivity between "brain" and "stroke". If it is chosen the use of a realistic phantom, one can find some recipes on literature. [40] has proposed successfully a brain phantom consisting on water, sugar and agar-agar. The same researchers in [41] suggest replacing agar-agar for plant gelatin because the previous material has exudation problems.

Pre-processing

Typically, in addition to the desired signals, there is a large quantity of noise. That noise is product of reflections from other objects belonging to the environment around the object of interest. To eliminate the noise, some pre-processing techniques were proposed in [42]. Both consisted on differences between measurements done with the antennas in certain positions and both proved to be successful. Another way of easing processing is the use of a bandpass filter (BPF) [43]. Using a BPF, it is possible to suppress the unwanted parts of the spectrum, where there is only noise, and thus helps an accurate stroke detection.

Processing

After measurements and pre-processing, it is necessary to analyze the resulting signals. A simple and efficient process for doing that is named DAS (delay and sum), which consists on assigning appropriate delays in order to the beamformer's focus steer on a specific point [34]. Futhermore, adding weighting coefficients called Coherence Factors (CF) improves resolution of the traditional method.

Instead of complete imaging reconstruction as the previously referred method, we can just determine which case is happening, which is our desired goal. A great way of achieving that is using classifiers. [31] refers the use of a particular classifier called Subspace Distance (SD), which is suitable when the dimension of the measured data is greater than the number of available samples and when the number of samples from one class is larger than other class. Separation between classes, healthy and with hemorrhagic stroke, is done based on defined thresholds, in

other words, if the value of the classifier is greater than a determined threshold then we are in the presence of a hemorrhagic stroke. They also concluded that the value for the classifier increases with the amount of bleeding.

3.2 Breast Cancer

Breast cancer is another disease where Microwave Imaging can make a difference. Based on the dielectric contrast between malignant and healthy tissue, it is possible to identify the tumor.

When Dielectric Contrast is not enough

As shown in [44], sometimes the contrast between malignant and healthy tissue is not so high. Considering that, using the electrical properties alone cannot guarantee high precision. To achieve a better result, another dimension is needed.

It is also known that the elasticity properties of tumors are different from normal healthy tissue. So, based on both differentiating characteristics, A.Abbosh and S.Cozier presented an approach consisting on applying UWB signals with compression of a breast and without compression. In each situation they saved the backscattered data and using both signals they obtained a three-dimensional strain image of the breast. The system used by them was composed by two plates, which compressed the breast. The antenna array was added to the top plate. In order to protect the antennas and achieve a perfect matching between antennas and breast tissue, they have added a superstrate layer with a dielectric constant equal to the average dielectric constant of the breast tissue (same problem as referred in strokes section). The detection was possible using the cross-correlation between both situations. If the tissue is healthy, the cross-correlation will reveal uniform displacement of tissues and in the case of tumor the displacement variation will be very low or even zero. The experimental results were achieved using CST Microwave Studio and frequencies between 2 and 12 GHz.

The plates in the previous example also played an important role preventing breast motion. As referred in [4], motion causes image blurring and consequently reduces sensitivity and resolution of the image procedure. Natalia K. Nikolova refers also another way of preventing motion, which is prone positioning, in other words, lying face down against the examination table (similar procedure as in MRI examination).

In [4], an explanation about in which cases there is enough contrast or not between malignant and healthy tissue is done. If the tumor is surrounded by fatty breast tissue, then the contrast between those two types of tissue is as large as 10. But if the tumor is enclosed by fibroglandular tissue (which is the more common case), then the contrast is not so high and we face a situation as described in [44]. It is also pointed out the possibility of injecting a contrast agent in the patient's blood stream in order to obtain greater image quality (procedure usually done in breast MRI).

Important Factors

There are several factors to consider when designing a system to detect breast cancer (also present in [4]):

1. The patient positioning
2. The use of coupling liquids
3. The acquisition surface
4. The type of acquired signals

Best Position for Acquisition

The best position for Microwave Imaging is the previously described prone position. That is due to a reduction of the movement of the breast during breathing. In this position, the breast is pendant through an opening in the examination table and may or may not be suspended in a tank of coupling liquid. [45] shows that it is not always the case. Two possible configurations are considered. The first configuration involves the patient lying in the supine (or face-up) position, where an antenna array is placed near the naturally flattened breast. This configuration allows for easier access to smaller breast volumes and tumors adjacent to the chest wall. The second configuration involves the patient lying in the prone (or face-down) position, with the breast extending through an opening in a treatment table. In this position, the antenna array encircles or in some other manner surrounds the pendolous breast. This configuration allows for easier access to the full volume of the breast.

Acquisition Surfaces

Relatively to the acquisition surface, there are three different options: planar, cylindrical and hemispherical surfaces. Depending on the position of the patient some of them are more suitable than the others. For example, cylindrical surfaces are usually used with the prone patient positioning where the breast is immersed in a tank of the coupling liquid and planar surfaces can be used independently of the position.

Radar Architecture

Concerning the radar architecture, there is also more than one single way of projecting the system. It is possible to use the reflected/backscattered signals using a single antenna to send and receive the signals, what is called of a monostatic radar, however, just a single backscattered signal is insufficient to image a living tissue. Considering that, usually it is used an array of antennas, in order to use confocal imaging approaches. Another possibility is to use only the transmitted signals to analyze the living tissue. As it is generally done in X-Rays, the analysis can also be done considering the different attenuation induced by the different tissues.

Processing Challenges

Scattering response at the skin-breast interface is more than one order of magnitude larger than any tumor response [45]. That is due to the high mismatch in dielectric properties between those two. So, in order to detect and locate correctly a tumor, it is mandatory to remove or suppress the signals correspondent to that unwanted scattering response without distorting too much tumor responses. The same article refers ways of overcoming the problem, for example via early-time artifact removal algorithm.

From high-cost to low-cost

As said before, to turn microwave imaging into a mass screening diagnostic tool, it is necessary to replace the bulky and expensive VNA with low-cost technologies. In that way, [4] proposes a low-cost dedicated CMOS integrated circuit. With that purpose in mind, they have developed a 65-nm CMOS receiver operating from 1.75 GHz to 15 GHz, which proved to be adequate to detect even the smallest tumors.

3.3 Heart Failures

Principle of Detection

Heart failures are followed by an accumulation of water in the lungs, what is called of Pulmonary Edema. That symptom allows the detection of a heart failure by the use of Microwave Imaging, which is possible because microwave energy is absorbed more in tissue with higher water content than in tissue with low water content. The key parameters to monitor are then, reflection and transmission measurements of the lungs, as both are sensitive to changes in lung water content.

Frequency Range

In order to determine the most suitable range of frequencies for detecting heart failures, Rezaeieh *et al* applied a simulation procedure described in [46]. They have represented each of the tissues involved as layers defined as lossy transmission lines. The characteristic impedance, electrical length and loss tangent of each equivalent transmission line was computed based on the dielectric constant and conductivity of each tissue type.

The frequency-dependent properties of the tissues are described in Table 3.2. At the skin layer, it is assumed a coupling medium and representing free-space they have used a termination resistor of 377 Ω.

After designing the complete system, they have calculated the amplitude of the signal that penetrates to the center of the lungs across the frequency band of interest considering the two different cases, with inflated or deflated lungs. As expected, they conclude that attenuation increases with an increase in frequency, however, using a proper coupling medium (of dielectric constant of 30 and 15 mm of thickness) the attenuation decreases across the band from 0.5 GHz to 1 GHz. To verify through simulation those results, they have used HFSS full-wave simulations.

Tissue	Dielectric constant	Thickness (mm)	Conductivity (S/m)
Skin	51	2	2
Fat	6	20	0.2
Muscle	18	48	1
Lungs (deflated)	53	140	0.7
Lungs (inflated)	22	140	0.35

Table 3.2: Frequency-dependent properties of tissues for a standard average person

Experimental Setups

Detections of the amount of water present in lungs have already been studied in 1978 [47]. Here, they recognized changes in the permittivity and conductivity of the lung tissue caused by the accumulation of water. Consequently, those changes affect microwave reflection and transmission characteristics.

One of the experiments made in [47] was artificially inducing edema in dogs at the same time as they were monitoring their chests. To do that, they have used a single-frequency reflection technique, with a frequency of 915 MHz. It is easy to identify the correlation between the amplitude of the reflection coefficient and the amount of water inside lungs in Figure 3.5. As the time goes by, there is progress in the edema state and the amount of water increases. The monitoring potential of single-frequency microwave reflection technique was shown here.

In [48], it is pointed out the limitation of a system consisting in the previously explained design. The study of the changes in the amplitude of reflected or transmitted signals is sensitive to the position of the measuring setup as well as the surrounding medium. To overcome that limitation, they have proposed a method consisting on sending and receiving wideband signals into the torso but using a differential technique expressed by a comparison between the scattering profile of the left and right side lungs. To differentiate between healthy and unhealthy cases they proposed a threshold, defined after experiments using realistic phantoms. The range of frequencies used was 0.77 - 1 GHz and the system was composed by a laptop PC, a Microwave transceiver and an unidirectional antenna. The data analysis was done with a script of MATLAB.

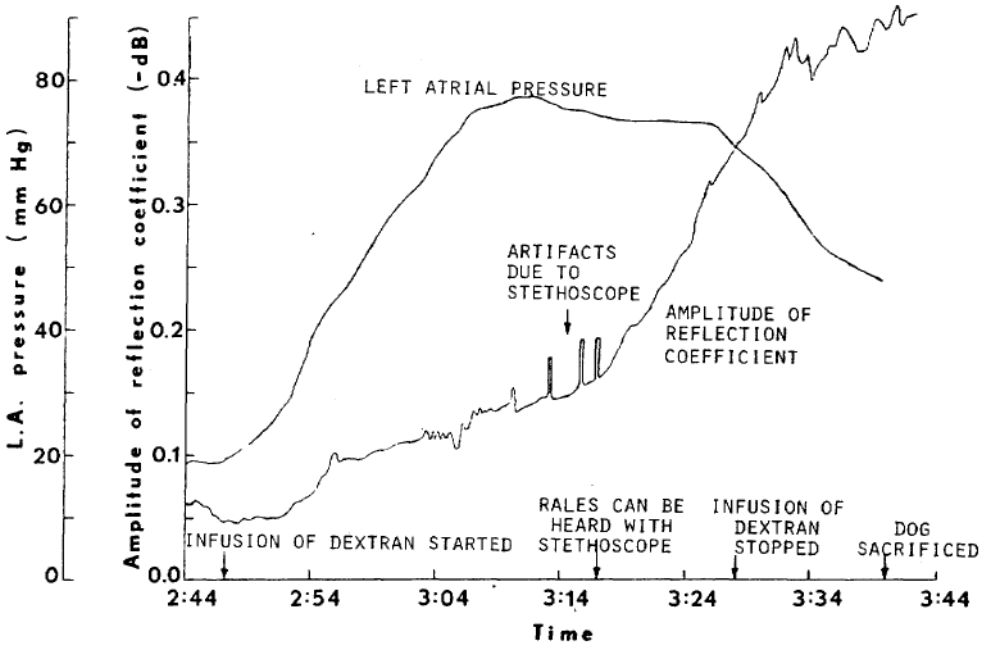

Figure 3.5: Reflection Coefficient vs Water Content Inside Lungs. Taken from [47]

3.4 SDRadar and Biomedical Applications

Previously, the importance of Microwave Imaging was demonstrated. In order to reduce the cost involved and improve the portability of the system, a Software Defined Radar arises as an important tool.

In this section, we will present a literature review on Software Defined Radar and its biomedical applications.

3.4.1 Software Defined Radar

In order to detect objects of interest one can use Radio Waves. The technology that allows this goal is called RADAR (Radio Detection and Ranging).

The first step into the "Radar world" was made by the German physicist Heinrich Hertz in 1886 [49], who showed that radio waves reflect when they encounter solid objects. Since then, several developments were made and today this technology is well known and fundamental to our daily life.

Radar's applications are extremely diverse. In the military operations, it plays a major rule because of its capability of detecting objects independently of the weather and hour of the day and, for the same reason, it is used in airports, allowing a safe navigation of airplanes.

In the recent years, the automotive industry became interested in the development of a fully autonomous vehicle. To accomplish that goal, a Radar in each vehicle is essential in order to avoid collisions. The same principle can be applied to UAV (Unmanned aerial vehicles).

All those new trends boosted the development of Radars until arriving what is called as Software-Defined Radar.

Traditionally, a radar system uses dedicated hardware, such as ASIC-circuits [50], which is developed for a particular task and is not reconfigurable. A Software-Defined Radar, instead, uses programmable devices, such as Field Programmable Gate Arrays (FPGAs) and computers, making possible to use one single radar in many applications.

The principle involved is simple. Previously, all the tasks were done in the hardware domain. With SDRadar, apart from Antennas, Digital-to-Analog Converters (DACs) and Analog-to-Digital Converters (ADCs), everything else is done in the software domain allowing an easy and fast reconfigurability of the system [51] [52] [53]. When considering complex applications with high frequencies involved, two more blocks are necessary for the system to work correctly, a mixing stage called RF front-end and a FPGA. The mixing stage, when receiving a signal, performs a down-conversion, in other words, converts a high frequency signal (RF) to a lower frequency, which could be an intermediate frequency (IF) or Base-band (BB) depending on the configuration used. When transmitting a signal, the process is inverted, a signal in IF or BB is translated to a RF carrier. The FPGA is used in order to reduce the computational burden of the computer when processing the signals.

The most efficient way of implementing a SDRadar is using the computer as the major processing unit [50]. When using the FPGA as principal unit of signal processing, the implementation of

the radar algorithm becomes limited to the number of logic blocks and memory elements present on the FPGA. But, using the computer to take care of most of the processing, the FPGA is only responsible for simple operations as decimation, and the SDRadar limit becomes only the processing speed of the computer.

Compared to "traditional" radars, Software Defined Radars have several advantages, namely, the possibility to use one single radar to various purposes, a faster development of complex signal processing algorithms and a reduced price.

An important requirement for SDRadar, related with the multipurpose capability of the system, is the use of wideband or multiband antennas.

3.4.2 SDRadar for Medical Imaging

Usually, as referred on previous sections, a VNA is used as a transceiver. It is a very effective device, however, it is also very expensive and heavy. In order to increase portability and reduce cost, it is necessary the use of a small and low-cost tool as a Software Defined Radio.

Appearance

Marimuthu *et al* proposed in 2014 the first imaging system based on SDR with medical purposes [54].

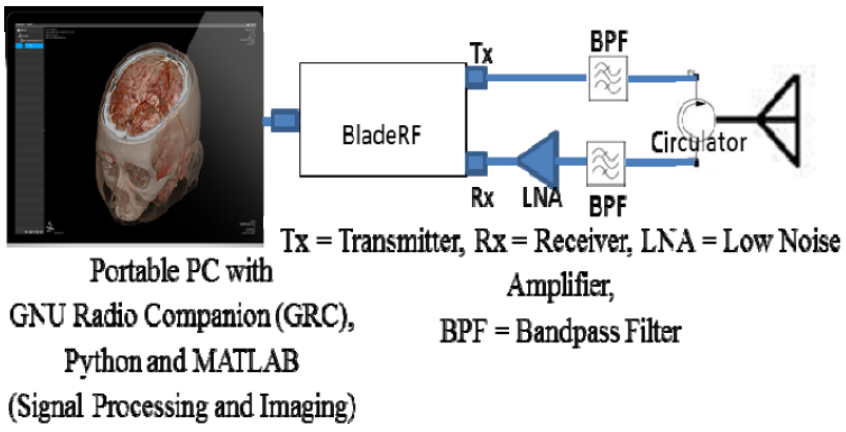

Figure 3.6: Complete design of the system proposed. Taken from [54]

They choose Blade-RF as their software defined radio board, arguing that for Medical Imaging it is the most suitable one. To manipulate the digital data, they have used GNU Radio Software, which was described in the first chapter of this document. Using both elements, they have designed a Stepped Frequency Continuous Wave Software-Defined radar and a Stepped Frequency Gaussian Noise Radar. The first one was capable of transmitting signals in the frequency range of 300 MHz - 3.5 GHz, with a stepping size of 30 MHz and RF output power of 0 dBm and the second one worked in the frequency range of 350 MHz - 3.5 GHz, with an identical stepping size as the previous implementation and with an output power dependent on the amplitude of the source. As

was seen on the previous sections, that range of frequencies is well-suited for medical imaging regarding the detection of strokes or heart failures.

Methodologies

Later, in 2015, the same researchers put into practice the previously developed SF-Continuous Wave SDR algorithm [55]. Using an RF front-end consisting on a circulator and a single tapered slot antenna they were able to transmit and receive signals in a monostatic approach. Due to the bandwidth limitations of the circulator, their system worked in the frequency-range 1.2 GHz - 2.2 GHz. In order to image and locate the abnormalities, they have used a rotating platform. To test the system, a phantom material with $\varepsilon_r = 7.1$ and targets with $\varepsilon_r = 77$ (water) were used.

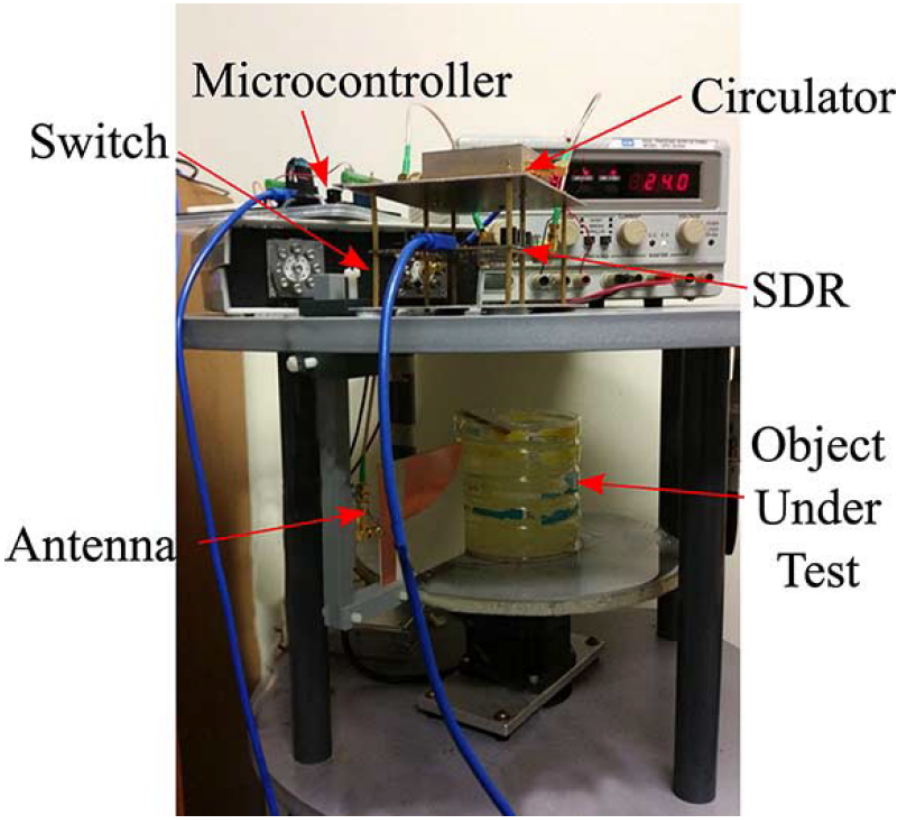

Figure 3.7: Experimental Setup. Taken from [56]

As shown in Figure 3.7, the phantom material was inside a plastic container. In [56], instead of the phantom material previously used, they tried canola oil ([55]) maintaining the water targets. In order to understand the behaviour of the system with phantom and targets closer in dielectric properties, they also used phantoms of $\varepsilon_r = 21$ and $\varepsilon_r = 45$. All of the results obtained were promising.

3.5 Discussion

Currently, Microwave Medical Imaging is under intensive research, which is due to its non-ionizing nature, accurate results, low-cost potential and possible areas of application.

In this Chapter, it was explained how a system using microwaves can be used to identify the type of stroke, detect breast cancer or pulmonary edema.

As pointed out in the preceding sections, a VNA is usually used as the system's transceiver. However, in the last two years a group of researchers from the University of Queensland in Australia have proposed to change the bulky and expensive VNA for a SDR. SDRadar for Medical Imaging is therefore an extremely recent topic and as was possible to identify in the previous section, there is not enough work done on that. As it can represent a fundamental role in future medical imaging systems due to its portability and low-cost, the research and development of this topic is of major importance.

Chapter 4

SDR Software and Hardware Platforms

4.1 Introduction

As referred in the previous chapter, the principle behind Software Defined Radio/Software Defined Radar is the translation of the modulation and demodulation of a signal from the hardware domain to the software domain.

In this dissertation, GNU Radio will be used as the Software Platform. In order to achieve a SDR capable of emitting and receiving real signals, it was necessary the addition of a Hardware Platform (Universal Software Radio Peripheral B200, in this case).

In this chapter an overview of the current software and hardware platforms available on the market will be given.

4.2 Software Platforms

We can find quite a few different software platforms for Software Defined Radios. However, some of them are designed for a particular operative system.

If we are using Windows as the operative system, SDR#, HDSDR and SDR-Radio are excellent choices since all of them are free and general-purpose [57].

SDR# is one of the most popular software platforms due to its simplicity of use. It includes a standard FFT display and waterfall, a frequency manager, recording plug-in and a digital noise reduction plug-in. Furthermore, many more plug-ins developed by third-party developers can be added.

HDSDR has also the standard FFT display and Waterfall. Moreover, it includes other features, e.g. noise reduction and filtering capabilities.

SDR-Radio is more difficult to learn than the previous examples but on the other hand offers also more advanced features.

However, whereas research purposes are intended, GNU Radio arises as the major player [57].

4.2.1 GNU Radio

GNU Radio is a free software development toolkit that provides signal processing blocks to implement software radios [5]. Combined with dedicated hardware such as, Universal Software Radio Peripheral (USRP), allows the implementation of a low-cost Software-Defined Radar.

GNU Radio has many elements normally included in Radio Systems such as filters, modulators, demodulators, channel codes and decoders.

The application consists of a flow graph [58] consisting in vertices composed by signal sources, sinks and processing blocks. Each block is characterized by the number of inputs and outputs and the type of data that it can process.

It is possible to find an enormous diversity of blocks. Some examples are given [58]: Mathematical Operations, Filters (FIT,IIR,Hilbert,ect.), Modulation and Demodulation (FM, AM, PSK, QAM, OFDM, etc.), Interpolation and decimation, signal generators, noise generators, Pseudo random number generators, Graphical sinks and several more.

There is also the possibility to introduce even more blocks. That can be done programming in C++. In order to build the graphs, Python is required.

As can be seen, GNU Radio allows a fast development of complex algorithms of signal processing, it is easily reconfigurable and completely free. Those characteristics make it suitable for the design of a low-cost SDR.

4.3 Different Hardware Platforms available on the market

There are several different hardware platforms being produced. Depending on the application required or the budget accessible one can choose the most suitable one.

RTL-SDR is a generic term for cheap USB digital TV (DVB-T) receivers that use Realtek RTL2832U chipset [59]. It is the cheapest hardware platform available ($10 to 22 USD) and even so, it is capable of operating at a satisfactory large frequency range (from 24 MHz to 1766 MHz) [59]. RTL-SDR major faults are its 8 bits ADC Resolution, its short real-time bandwidth (3 MHz) and the impossibility of transmitting signals.

In Table 4.1, three Software Defined Radios only capable of receiving signals but better and also more expensive than RTL-SDR are presented.

Platform	**SDRPlay RSP**	**Airspy**	**FunCube Dongle Pro +**
Cost	$150	$199	$210
Frequency Range	100 KHz - 2 GHz	24 MHz - 1.750 GHz	410 MHz - 2.05 GHz
Max. Sample Rate	10.66 MS/s	80 MS/s	192 KS/s
ADC Resolution	12 bits (10.4 ENOB)	12 bits (10.4 ENOB)	16 bits
Max. Bandwidth	8 MHz	10 MHz (9 MHz alias free)	80 KHz
TX/RX	Rx only	Rx only	Rx only

Table 4.1: Comparison between receive only platforms

Since for sensing as well as imaging purposes, it is necessary transmission and reception of signals, the SDRs shown in Table 4.1 are not useful. Table 4.2 compares Software Defined Radios capable of transmitting and receiving in a full-duplex mode, which means that they can transmit and receive simultaneously. Not included in the table but probably the most famous SDR due to the educational videos of Michael Ossmann [60] is HackRF one. Though HackRF is capable of transmitting and receiving, it does that in a half-duplex mode, in other words, it is capable of doing both but not simultaneously. And that makes it unsuitable for Microwave Medical Imaging.

Platform	**BladeRF**	**MyriadRF**	**USRP B200**
Cost	$650	$299	$675
Frequency Range	300 MHz - 3.8 GHz	300 MHz - 3.8 GHz	70 MHz - 6 GHz
Max. Sample Rate	40 MS/s	15.36 MS/s	61.44 MS/s
ADC Resolution	12 bits	12 bits	12 bits
Max. Bandwidth	28 MHz	28 MHz	56 MHz
TX/RX	Tx and Rx (Full duplex)	Tx and Rx (Full duplex)	Tx and Rx (Full duplex)

Table 4.2: Comparison between full duplex platforms

4.4 USRP B200 vs BladeRF

As pointed out in Chapter 3, all the experiences made in the medical domain with a Software Defined Radio were done with a BladeRF. It makes sense then, to compare in more detail the BladeRF with the USRP B200 (SDR used in this dissertation).

BladeRF offers a wide range of frequency operation proper for medical imaging (300 MHz to 3.8 GHz) and it is even possible to extend the same to lower frequencies with an additional transceiver module [61]. It has independent Rx and Tx signal paths, which allows full duplex operation and makes possible to define frequency, sample rate, bandwidth and gain differently for transmission and reception. It works being powered over USB 3.0 or using USB 2.0 with external power source. GNU Radio can interact with the platform via gr osmosdr. In addition to GNU Radio, BladeRF is supported by SDR# and Matlab & Simulink.

USRP B200 has many characteristics identical to BladeRF, namely, full-duplex mode of operation, 12 bits of ADC resolution and USB bus powering. It is also supported by GNU Radio (osmosdr and UHD interfaces), SDR# and Matlab & Simulink. But, in addition, its performance is better in terms of RF coverage (70 MHz - 6 GHz vs. 300 MHz - 3.8 GHz), instantaneous bandwidth (56 MHz vs. 28 MHz) and sampling rate (61.44 MS/s vs. 40 MS/s).

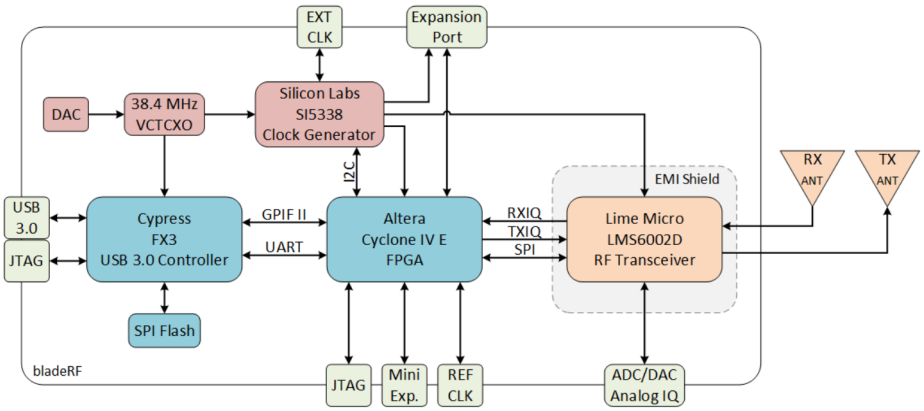

Figure 4.1: Building blocks of BladeRF. Taken from [61]

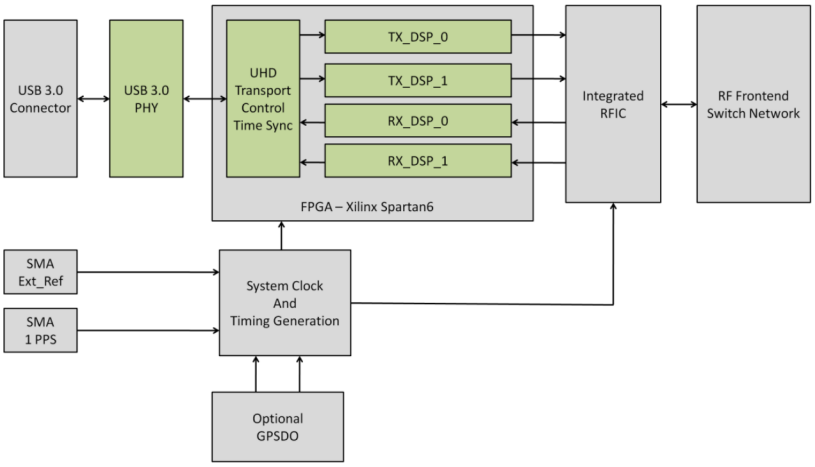

Figure 4.2: Building blocks of USRP B200. Taken from [6]

4.5 Discussion

There are several options available on the market, both for Software as well as Hardware platforms.

Regarding the Software platform, GNU Radio meets all our requirements. It is completely free, easily reconfigurable and allows a fast development of complex algorithms of signal processing. It is therefore an obvious choice.

The choice of the Hardware Platform is not so easy. USRP B200 has many interesting characteristics such as: working in the frequency range of interest, allowing full duplex operation, being powered over USB 3.0 and being supported by GNU Radio. However, it is a little bit costly when compared to other platforms and only allows the use of two antennas at the same time. Nevertheless, we consider that it offers the most cost-efficient solution.

Chapter 5

Development of a SDRadar human bio-sensing system prototype

5.1 Introduction

It is possible to measure vital signs, in this case respiration, taking advantage of the Doppler theory. When an electromagnetic wave is sent and hits a moving target (for instance, a moving chest), the backscattered wave is shifted in frequency (equation 5.1).

$$f_{received} = f_{transmitted} + f_{doppler} \tag{5.1}$$

The breathing cycle is characterized by two different phases, inhalation and exhalation. During inhalation oxygen enters the lungs to later be absorbed into the bloodstream. This process causes an approaching movement in relation to the antenna/system and consequently originates a positive doppler frequency. During exhalation, carbon dioxide and other gases are expelled causing a departure movement relative to the antenna and as a result a negative doppler frequency. Considering this, the number of breathing cycles can be calculated based on the number of transitions from positive doppler frequency to a negative doppler frequency.

5.2 System Description

In this section, the overall architecture of the system used for Respiration Monitoring is described. Each critical decision made is explained and the ideas for analysing the results are referred.

Hardware Platform

USRP B200 was the hardware platform used in this thesis as referred in Chapter 4. It was selected because it is one of the cheapest full duplex hardware platforms (Myriad RF is cheaper but by itself does not have hardware to connect to a PC) and because its frequency range of operation is well suited for the applications described in Chapter 3. Usually, the platform itself does not have a RF Front-End but the bus series from Ettus Research, where the USRP B200 belongs, is

an exception. Its integrated front-end does up- or down-conversion directly from base-band to RF, or vice versa, without intermediate frequency stages, which means that it works as a homodyne transceiver.

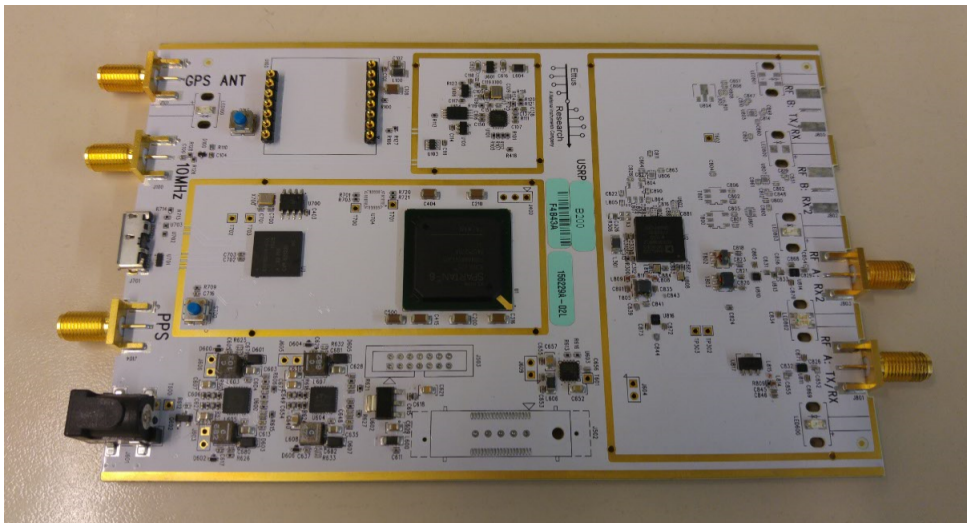

Figure 5.1: USRP B200

Software Development Toolkit

GNU Radio was used as the Software Development Toolkit. It was chosen because it is free and open source, allowing the goal of using a low-cost system. In addition to those characteristics, it is also characterized by high flexibility, in other words, it is possible to change the algorithm and consequently implement it in a question of seconds (if the algorithm was already designed). To even increase the flexibility of the total system it was used the GNU Radio Live SDR Environment [62], which makes the system independent from the Laptop and only requires an USB 2.0/3.0 port to run the operative system from the SSD card.

Transmission Antenna

As transmission antenna we have used a Log Periodic PCB antenna bought from [63]. It was chosen because of its frequency range of operation (850 MHz to 6.5 GHz), which is identical with the one from the USRP B200 (70 MHz to 6 GHz) allowing then multiple purposes (respiration monitoring and medical imaging). It has a gain of 5-6 dBi, which is sufficient to achieve the desired results and still be completely safe for human monitoring.

Reception Antenna

For reception purposes a Horn Antenna with 9 dB of gain (at 3 GHz) was used. It was already present in the Laboratory and it works from 2 GHz to 18 GHz. Since it is used for reception, its high gain is not a problem in terms of safety requirements.

Circulator

A circulator, as defined in [64], is a passive non-reciprocal three- or four-port device, in which a microwave or radio frequency signal entering any port is transmitted to the next port in rotation

(only). A port in this context is a point where an external waveguide or transmission line (such as a microstrip line or a coaxial cable), connects to the device. For a three-port circulator (our case), a signal applied to port 1 only comes out of port 2, a signal applied to port 2 only comes out of port 3 and a signal applied to port 3 only comes out of port 1. That property allows us to use just one antenna instead of two. In other words, transmission and reception are occurring through the same antenna at the same time and are separated by the circulator.

Since there was one circulator available in the Laboratory covering a frequency range from 2 GHz to 4 GHz, it was also used, allowing the system to work only with the Log Periodic PCB antenna.

Operation Frequency

In Chapter 2 a review on the literature was made and it was referred that there are examples of experiments from 1 GHz to 35 GHz or even higher frequencies. There are advantages and disadvantages on the selection of a higher or lower frequency. A high frequency of operation allows better resolution but it is worse in terms of operating distance and capacity of penetration of possible obstacles between the system and the object of interest (in this case, a person). The frequency of operation was selected considering both transmitting and receiving antennas, the hardware platform, the circulator available and the problem itself. So, in order to respect the frequency ranges of operation of all materials and since monitoring respiration does not require high resolution, an operation frequency of 3 GHz was chosen. It was taken into account all the noise at 2.4 GHz, namely Wi-Fi signals, and then frequencies near this one were not considered.

Sampling Frequency

The selected sampling frequency should follow the Shannon-Nyquist sampling theorem (5.2). In this particular problem, f_{max} is considered as the maximum doppler frequency induced by breathing. In order to define a reasonable value for f_{max} one can use equation (5.3), where v_r is the relative velocity of the target, f_o is the operation frequency and c_o is the velocity of the light. Assuming a maximum velocity of 5 m/sec [65] results a doppler frequency of 100 Hz (5.4), and consequently a minimum sampling frequency of 200 Samples/second.

$$f_{sampling} > 2 f_{max} \tag{5.2}$$

$$f_{doppler} = 2\frac{v_r f_o}{c_o} \tag{5.3}$$

$$f_{doppler} = 2 \times \frac{5 \times 3 \times 10^9}{3 \times 10^8} = 100 \tag{5.4}$$

Obviously, 5 m/s is too high for the breathing motion but even with this consideration, the resulting value for the doppler frequency and consequently for the sampling frequency is extremely low.

Transmit Power

The system's object of interest is a person and being so, it is necessary to guarantee his/her safety. [65] refers a limit of 39 dBm to the value of the EIRP if the system is closer than 0.5 m in relation to the person. This value is derived from the maximum power density allowed of 1 mW/cm^2 defined by the FCC (Federal Communications Comission).

Regarding that condition, the system should respect equation 5.5, where $G_{antenna}$ is the gain of the transmission antenna (dB), $P_{transmitted}$ is the power coming out from the hardware platform (dBm) and L_{cable} is the power lost in the cable used (a negative value in dB). However, it should be noted that this equation is only valid for far-field and that could not be the case. It will depend on frequency and distance between system and subject.

$$EIRP = G_{antenna} + P_{transmitted} + L_{cable} < 39 \tag{5.5}$$

General System Architecture

The complete system is described in Figures 5.2 and 5.3 . It consists of two antennas (Figure 5.2), or one antenna and one circulator (Figure 5.3), the USRP B200 and a Laptop with GNU Radio installed. The communication between the laptop and USRP B200 is made using GNU Radio Companion to define the desired parameters and USB 3.0 as transport vehicle of the information. Then, the hardware platform will send a continuous signal through the Tx antenna (Log Periodic PCB antenna) that will reach the person's moving chest. When the signal hits the chest, it will occur scattering and the backscattered signal will be collected by the Rx antenna (Horn Antenna) or by the same Log Periodic PCB antenna in the circulator case. Afterwards down-conversion will occur and the next processing steps will be done in GNU Radio.

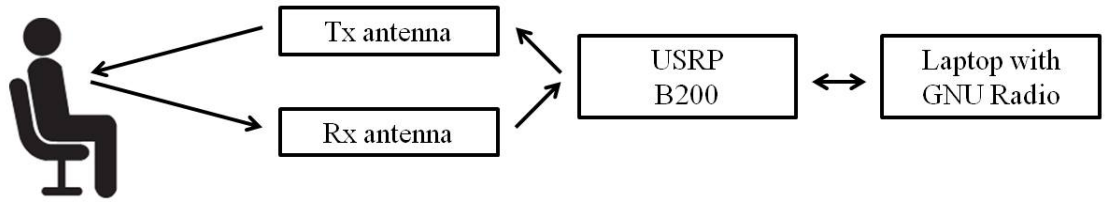

Figure 5.2: General System Architecture #1

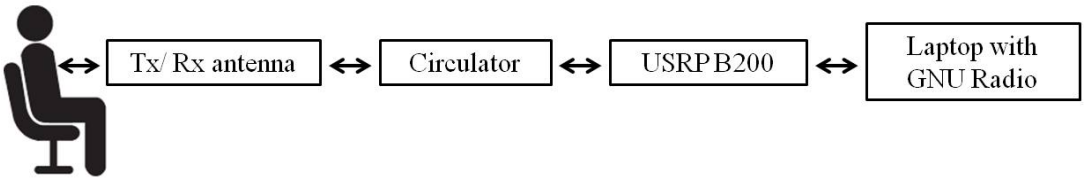

Figure 5.3: General System Architecture #2

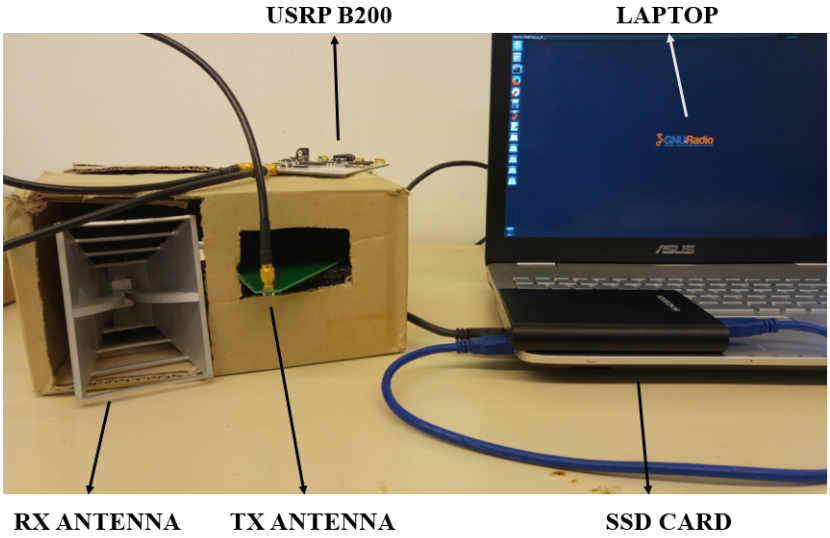

Figure 5.4: Experimental Setup for Architecture #1

Methodology

In order to observe breathing motion it is necessary to send a continuous signal and compare it with the resulting backscattered signal. If there is movement, the received frequency will differ from the transmitted one by a factor correspondent to the induced doppler frequency. Therefore, to understand what is going on, it is necessary to compute the value of that doppler frequency (Equation 5.6), since its signal contains information about the trajectory of the target. From signal theory we know that the multiplication of two sine waves (what is done by block "Multiply Conjugate") will result in the sum of two different sine waves, one characterized by a frequency equal to the sum of the previous frequencies and another characterized by the difference of the respective frequencies. So, after filtering the signal with a frequency correspondent to the sum of the previous ones, we have the desired signal (doppler signal). Finally, the signal is transformed from time domain to frequency domain by the Fast Fourier Transform (FFT).

$$f_{doppler} = f_{received} - f_{transmitted} \tag{5.6}$$

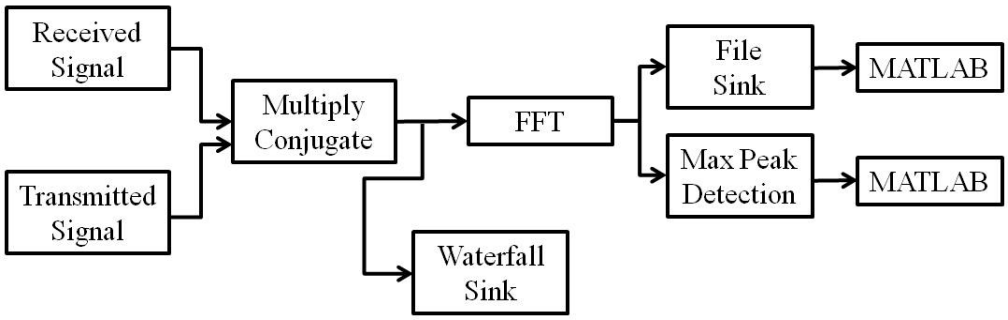

Figure 5.5: Algorithm for monitoring respiration and calculation of its frequency

Observation of breathing

To observe in real-time if a person is breathing or not, a Waterfall plot is used (Figure 5.6). As shown in Figure 5.5, the Waterfall Sink is previous to the FFT block. It is that way because the Waterfall Sink itself already computes the FFT operation before displaying the results.

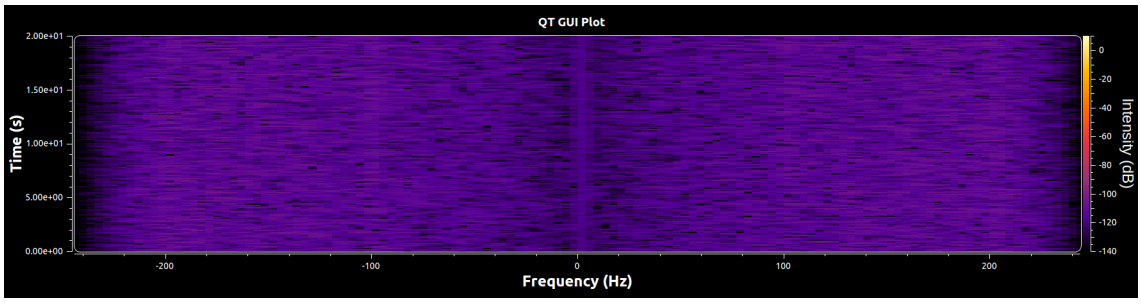

Figure 5.6: Waterfall without breathing

Determination of breathing's frequency

A script written in MATLAB will be used to determine respiration frequency. Frequency can be obtained considering the number of breathing cycles (N_{cycles}) and the observation time (Δt) (Equation 5.7). Each one of those two variables can be collected from GNU Radio.

$$f_{breathing} = \frac{N_{cycles}}{\Delta t} \tag{5.7}$$

After Max Peak Detection, values of the velocity peaks are recorded in a file. Some of the values are positive (corresponding to positive doppler frequencies) and some of them are negative (corresponding to negative doppler frequencies). That being said, one can determine the transitions from positive to negative velocities, in other words, the number of breathing cycles.

The observation time, on the other hand, is calculated based on the number of samples ($N_{samples}$) and on the sampling frequency ($f_{sampling}$) (Equation 5.8).

$$\Delta t = \frac{N_{samples}}{f_{sampling}} \tag{5.8}$$

5.3 Results

Once the implementation of the system was finished, several experimental tests were done. The goal was to determine if its performance corresponded to the proposed objectives. We will now analyze the results obtained.

The first thing that was done was measuring the power coming out from the hardware platform in order to be sure about the safety of the system. It was measured a value of -27.43 dBm in a Spectrum Analyzer (Figure 5.7). That value includes the power coming out from the USRP B200 ($P_{transmitted}$) and the cable losses (L_{cable}). Since we know the antenna's gain, it is possible to determine if the system respects equation 5.9. Considering a gain of 6 dB (Log Periodic PCB antenna), the total power is -21.43 dBm, a value that is much smaller than the limit proposed (39 dBm) [65]. However, this value is not exactly correct because we are working at a distance of 30 cm and, therefore, we are not yet at far-field. Anyway, it works as a valid reference for safety requirements.

$$EIRP = G_{antenna} - 27.43 < 39 \tag{5.9}$$

After ensuring the safety of the system, a set of experiments was performed (Figure 5.8). All the tests were executed with a person sitting in front of the box with the antennas inside as shown in Figure 5.4.

As said in the previous section, the system was designed with real-time observation in mind. During the experimental tests, it was possible to verify that the system monitors respiration properly. Figure 5.9 illustrates the resulting Waterfall plot when there is a continuous and normal breathing cycle. In order to find out if the system was also able to detect interruptions of the normal breathing motion, it was done a period of observation with the person holding breath for two times. The resulting plot is shown in Figure 5.10, where it is possible to see correctly both interruptions.

After knowing that the observation of breathing was successful, the next step was to test the algorithm designed for computation of the frequency. The algorithm, as referred previously, works considering the number of transitions from positive to negative doppler/relative velocity and the observation time.

The number of breathing cycles is computed based on the resulting values from Max Peak Detection. Figure 5.11 shows a plot consisting on those resulting values. Then, applying an algorithm to calculate the transitions we obtain the value of breathing cycles (19 in the figure's case).

Next, the observation time is determined using equation 5.10. As shown in Figure 5.5, after the computation of the FFT, a binary file will store all the resulting values. Since what we are storing are complex numbers, the I (in-phase) and Q (quadrature) samples are interleaved and the number of *floats* (N_{values}) in the file is twice the number of samples ($N_{samples}$).

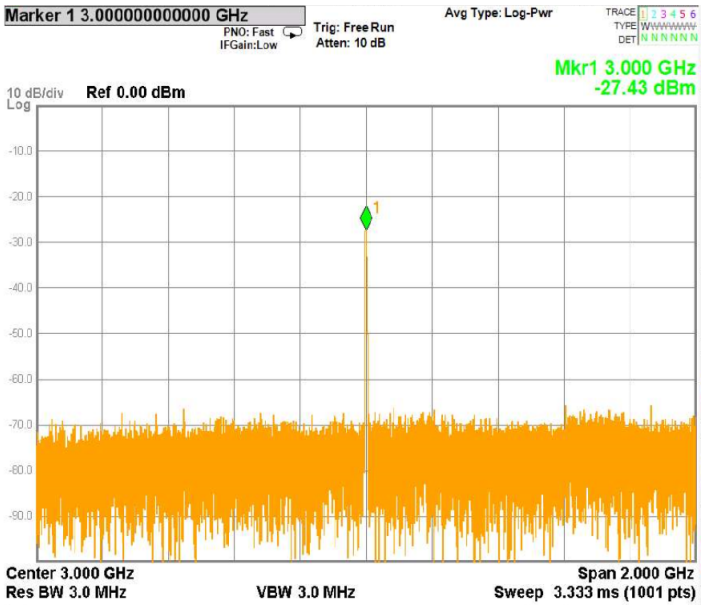

Figure 5.7: Transmitted Power including cable losses - Doppler Radar

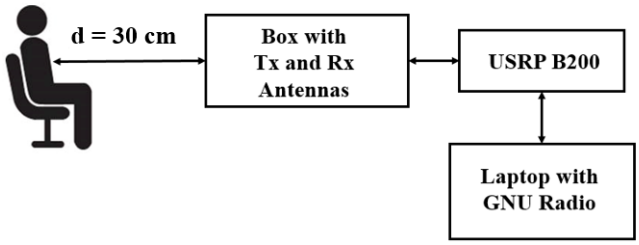

Figure 5.8: Experimental Setup for Architecture #1

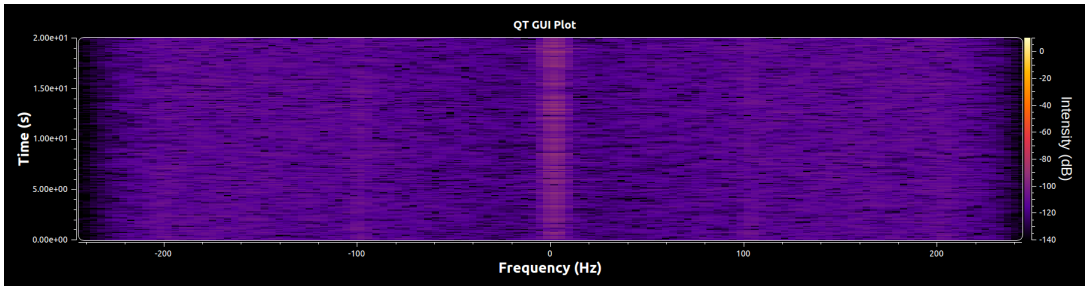

Figure 5.9: Waterfall with constant breathing

$$\Delta t = \frac{N_{samples}}{f_{sampling}} = \frac{N_{values}}{2 \times f_{sampling}} \tag{5.10}$$

Regarding the experiment example (considered in Figure 5.11), we have 62976 *floats* saved in the binary file. So, we can conclude that the number of samples is 31488 (Equation 5.11).

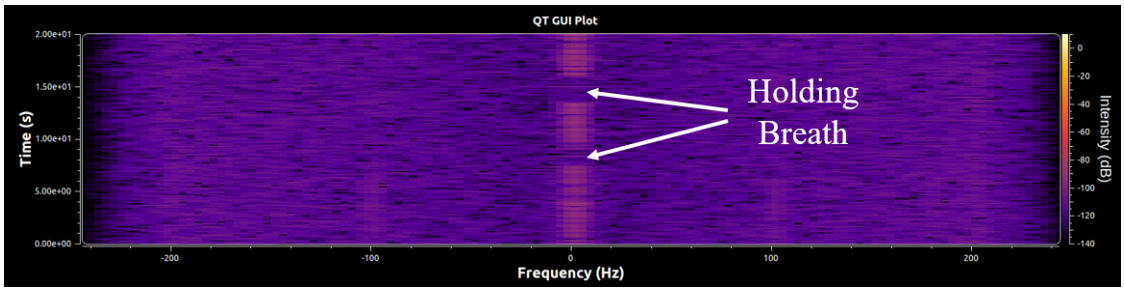

Figure 5.10: Waterfall with two interruptions. Each interruption is consequence of holding breath

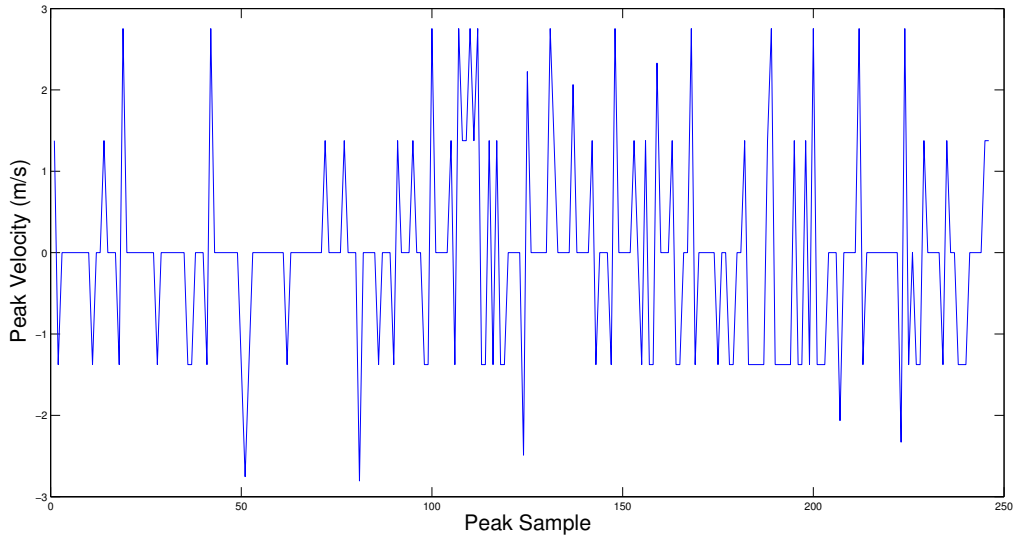

Figure 5.11: Representation of Max Peak Results

$$N_{samples} = \frac{N_{values}}{2} = 31488 \tag{5.11}$$

Since the sampling frequency of our system at the time of the FFT computation is 488 Samples/s, it is already possible to determine the value of the observation time (Equation 5.12) and consequently breathing frequency (Equation 5.13).

$$\Delta t = \frac{N_{samples}}{f_{sampling}} = \frac{31488}{488} \approx 64.52 \tag{5.12}$$

$$f_{breathing} = \frac{N_{cycles}}{\Delta t} = \frac{19}{64.5} \approx 0.29 \tag{5.13}$$

In Table 5.1, the results from this experiment example and from two additional experiments are presented. These three experiments were performed in different days and with variable observation times. However, they were performed with the same person and always with a distance of 30 cm between box with antennas and subject's chest.

Experiment	Samples	Obs. Time (s)	Breathing Cycles	Breathing Frequency (Hz)
1st	31488	64.52	19	0.29
2nd	65152	133.51	54	0.40
3rd	21248	43.54	12	0.28

Table 5.1: Experimental Results

5.4 Discussion

In this Chapter, system description and results about respiration monitoring were presented.

A breathing frequency of 0.29 Hz was obtained in the experiment example shown. This value is inside the frequency range exposed in literature (0.1 - 0.8 Hz) [17] and the same is true for the other two experiments performed.

To validate our breathing frequency, we have considered the number of breathing cycles and the observation time. The number of breathing cycles was verified counting each cycle while doing the experiment. In turn, observation time was confirmed using cell phone's clock. Doing that, we conclude that our algorithm is very precise, allowing us to determine the correct values.

However, to obtain the correct results, the subject of observation needs to be completely quiet. Any movement beyond breathing motion can lead to a wrong calculation of the breathing frequency. That is due to the principle behind our algorithm. We are measuring movements and the system, which consists on a CW radar, is not able to differentiate the source of the movement. In other words, we consider every movement has being caused by the subject's chest.

Chapter 6

Development of a SDRadar medical imaging system prototype

6.1 Introduction

In this Chapter, it is explained the architecture of a system capable of identifying the presence or absence of an object with different electrical properties inside a phantom.

As explained in Chapter 3, it is possible to determine which kind of stroke a person has, based on the fact that a hemorrhagic stroke causes a change in the normal dielectric properties of a certain region of the brain. An ischemic stroke also causes a change in the dielectric properties but in a different manner. Then, it is possible to identify a stroke and to differentiate between both types using microwaves. Furthermore, the same principle apply for breast cancer and heart failures.

The detection principle is based on the electromagnetic theory. It is known that if a TEM (Transverse electromagnetic) wave hits a boundary between two different dielectrics, part of the initial wave will be reflected and the rest will be transmitted. The fraction of the incident power that is reflected is determined by the reflection coefficient (6.1), whereas the fraction of the incident power that is transmitted is determined by the transmission coefficient (6.2). Their values are calculated considering the characteristic impedance, η, of both dielectrics. In turn, the characteristic impedance depends on the values of the permeability (μ) and permittivity (ε) of the material (6.3). Usually, those material's properties are defined compared to the values of the free-space, being named of relative permeability (μ_r) and relative permittivity (ε_r), also known as dielectric constant.

$$r = \frac{E_{reflected}}{E_{incident}} = \frac{\eta_2 - \eta_1}{\eta_2 + \eta_1} \tag{6.1}$$

$$t = \frac{E_{transmitted}}{E_{incident}} = \frac{2 \times \eta_2}{\eta_2 + \eta_1} \tag{6.2}$$

$$\eta = \sqrt{\frac{\mu}{\varepsilon}} = \sqrt{\frac{\mu_o \mu_r}{\varepsilon_o \varepsilon_r}} = \eta_o \sqrt{\frac{\mu_r}{\varepsilon_r}} \tag{6.3}$$

6.2 System Description

This system is very similar to the previous one but the principle used is completely different. Instead of analyzing the difference in frequency between transmission and reception, here what matters is the received power. In this description, it will only be referred the aspects that differ from the the previous system.

Transmission and Reception Antennas

In this system, both transmission and reception antennas are Log Periodic PCB antennas. That is justified by their frequency range, which is much more adequate concerning the problem to solve than the frequency range of the horn antenna used before. As already mentioned, the horn antenna does not work for frequency values lower than 2 GHz and according to what is present on the literature review (Chapter 3), it is of great interest to investigate this lower frequencies.

Operating Frequency

Unlike the previous system, this one does not have a determined operating frequency. It was designed in a way that allows to scan a wide range of frequencies in real-time in order to find the most suitable one for identifying the presence of a target inside the phantom. Figure 6.1 illustrates the way of changing the operation's frequency value. Moving the bar correspondent to *center_freq*, we can select the frequency of operation and observe on the FFT plot if the same is suitable or not for the detection of the target.

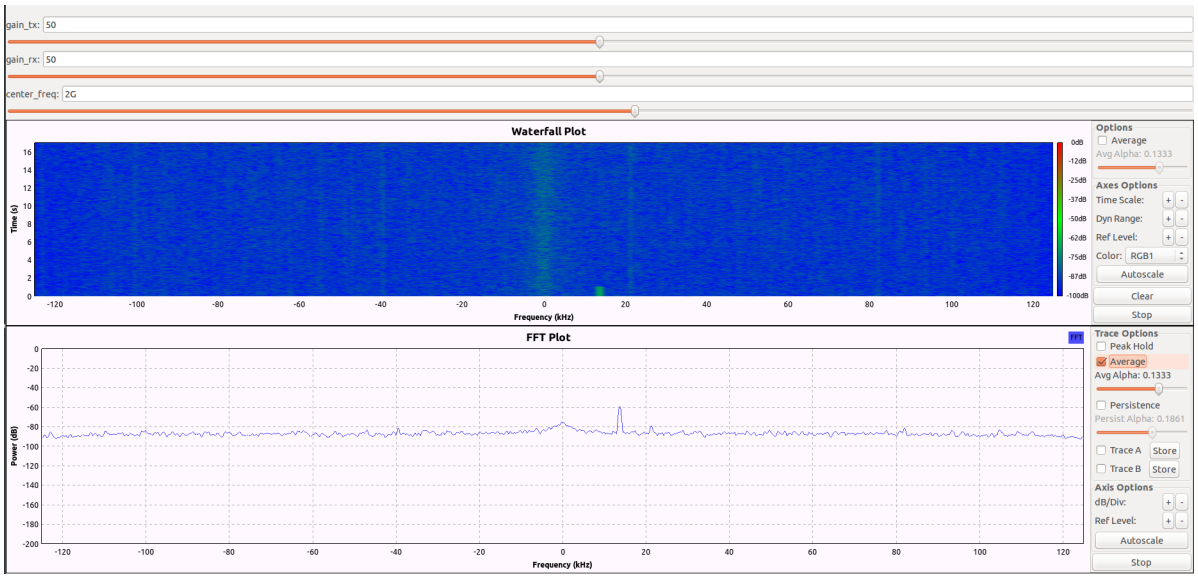

Figure 6.1: Interface for definition of operation's frequency and visualization of results

General System Architecture

Basically, this system uses the same architecture as the previous one. It is also constituted by a Laptop with GNU Radio installed, the USRP B200 and transmission and reception antennas. The difference is that the object of interest is no more a person's chest but a phantom simulating

the brain. Besides that, the location of the antennas could also not be the same, since we can be looking for a reflection or transmission value.

Methodology

The idea for detecting the presence of a target inside a phantom is to send a wave and then analyze the received power, which can be the transmitted part of the incident signal or its resulting reflected part. For that purpose, it will be sent a continuous sine wave (Figure 6.2) or gaussian noise (Figure 6.3, as proposed on [54]). The presence of a target will change the "normal" received power as a consequence of the theory explained before.

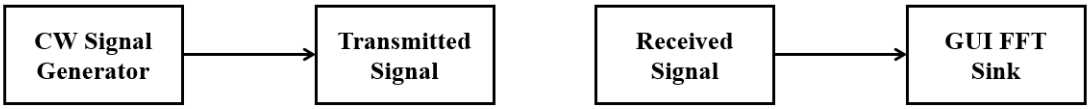

Figure 6.2: Algorithm using Continuous Wave

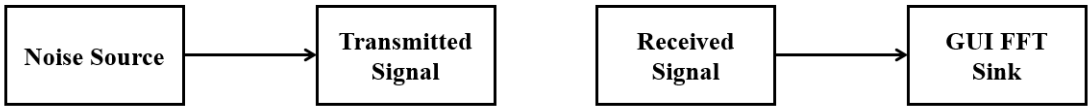

Figure 6.3: Algorithm using Noise Source

Reflection Configuration

In this configuration the position of the antennas will be identical to that of the respiration monitoring system (Figure 6.4). Here, the plan is to observe the difference in the power of the backscattered signal with and without the target. If a detectable difference is present then it is possible to identify an abnormality in dielectric properties with this system.

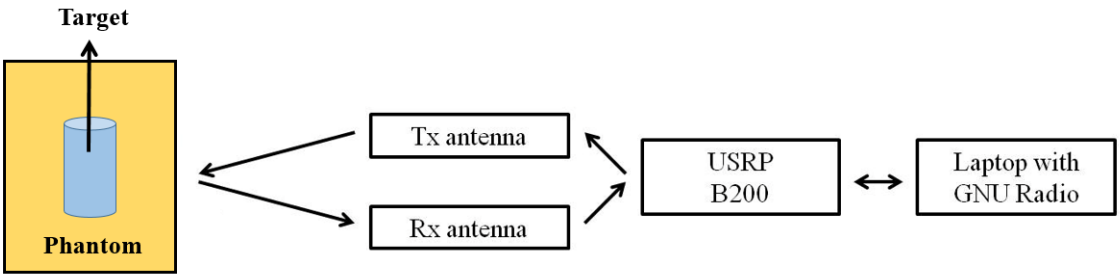

Figure 6.4: Reflection Configuration

Transmission Configuration

The same idea can be applied in a transmission configuration (Figure 6.5). As shown in Figure 6.6 and with more detail in Figure 6.7, there is one antenna on each side of the phantom. Hence, here what is analyzed is the transmitted part of the incident signal.

As exhibited in Figure 6.7, transmission antenna (Tx antenna) is on one side of the phantom and it sends the desired signal in the direction of the reception antenna (Rx antenna), which is located on the other side. Therefore, we make the most of the power that we send.

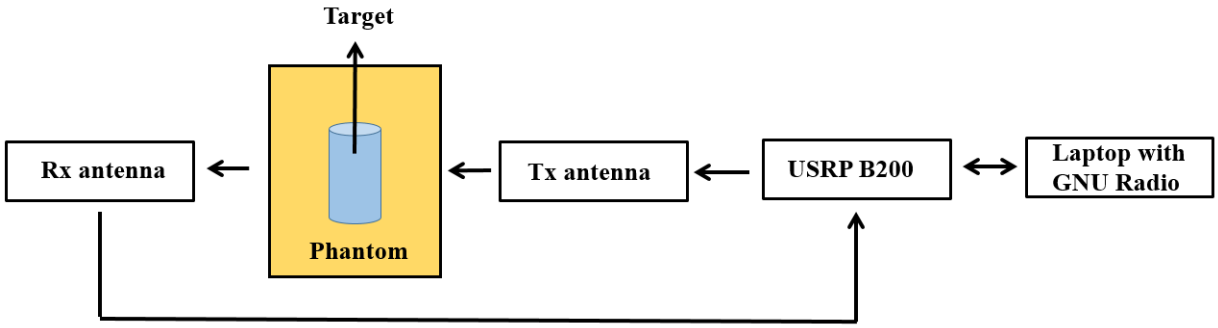

Figure 6.5: Transmission Configuration

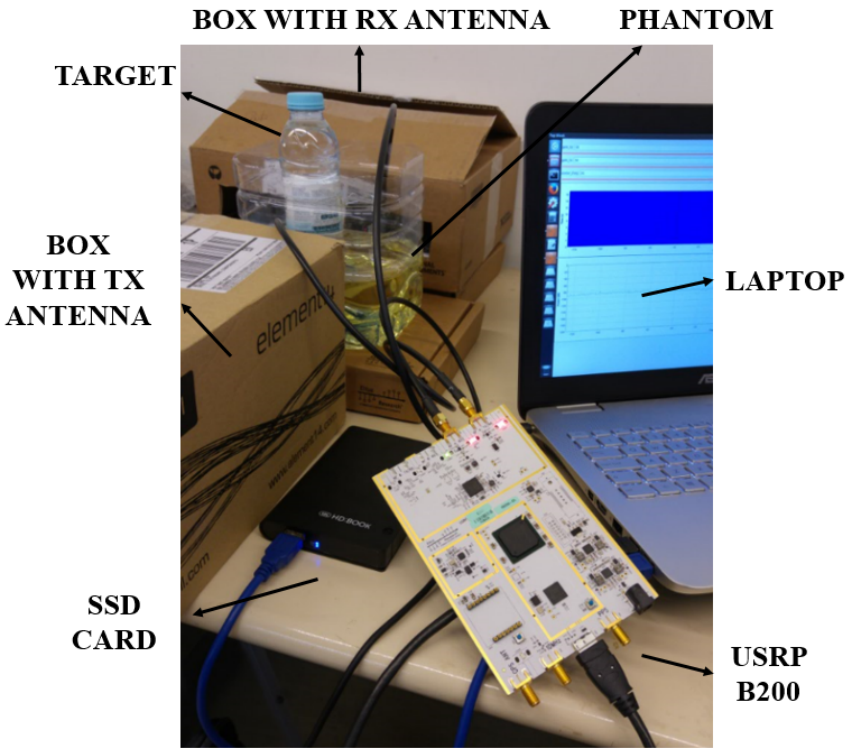

Figure 6.6: System for transmission measurements

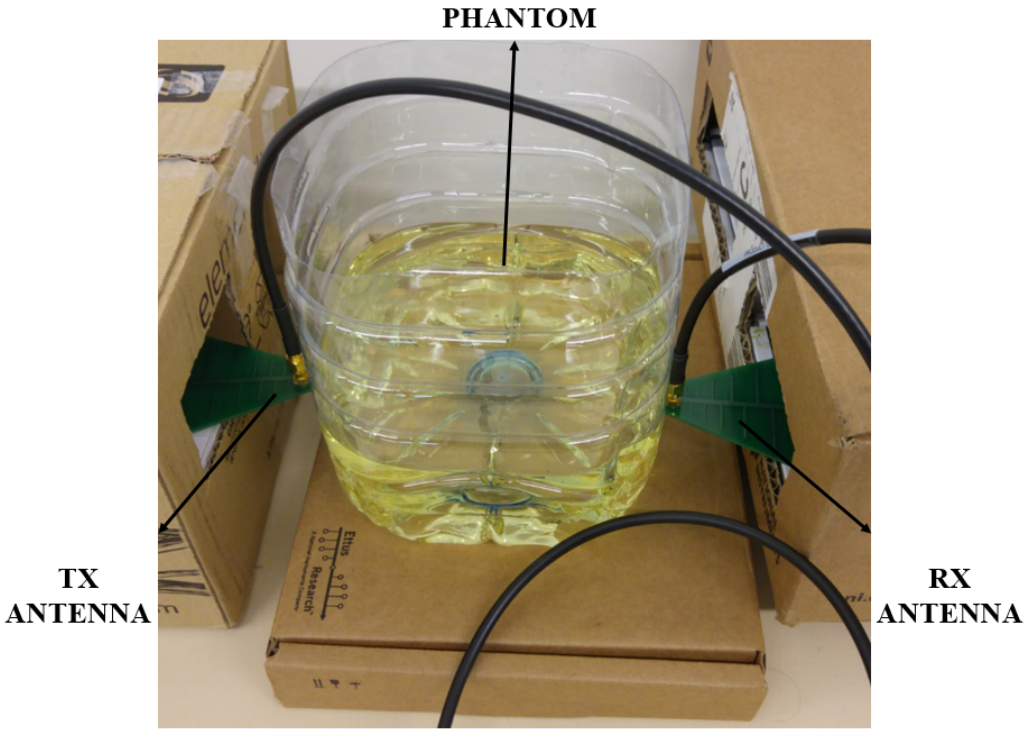

Figure 6.7: Close look to the transmission configuration

6.3 Results

Although tests are not done on humans (but on a phantom), the safety of the system was also considered. Since it consists on sending a continuous sinusoidal signal as in the previous system, and as we are maintain its gain, it is reasonable to say that safety is guaranteed despite the change in frequency.

Phantoms and Targets

In order to demonstrate the usefulness of this system, a set of measurements was performed using a plastic container firstly filled with sunflower oil (Figure 6.7) and afterwards with juice.

Regarding the target, we have started with a small bottle of water (33 cl), as can be seen in Figure 6.6, and to verify the resolution limits of the system proposed, we have finished our experiments using a syringe full of water (5 ml).

Reflection Configuration - Gaussian Noise based Software-Defined Radar

Following what was proposed on [54], a Gaussian Noise based SDRadar transmitter and receiver was designed by using GNU Radio Companion blocks. We have defined our parameters (Table 6.1) in a way that is similar to what they did. Thus, it is possible to scan the spectrum from 850 MHz to 3.5 GHz with a bandwidth of 25 MHz relative to each transmitting frequency.

Considering our goal of analyzing the reflected signal, the ideal situation would be to have a monostatic radar. That is due to the fact that in a monostatic configuration we would not lose

Parameter	Value
Amplitude of Gaussian Source	0.28
Sample Rate	62.5 KS/s
Center Frequency	0.85 GHz - 3.5 GHz
Bandwidth	25 MHz

Table 6.1: Gaussian Noise SDRadar Parameters

"information" to other directions apart from the Rx direction. However, both circulators available in the Laboratory work with frequencies outside the desired band, namely, 2 to 4 GHz and 3 to 5 GHz.

So, to observe how reflected power changes with the presence of a target, we approached the problem with a configuration, which is similar to that of the previous Respiration Monitoring system. In other words, Tx and Rx antennas were positioned so that both were directed to the target (Figure 6.8). In this experimental case (Figure 6.9), the wall works as a possible plate located at the opposite side of the antennas and is the medium responsible for the main reflection.

As previously stated, the initial experiments were done using sunflower oil (phantom) and a small bottle of water (target). Figure 6.10 shows the difference in received power between the case without the target (red - A) and with it (purple - B). After introducing the water target, we can consider that reflection occurs twice, i.e. one reflection occurs before encountering the wall and another occurs after being reflected on the wall. Those events will induce a reduction in the power received by Rx Antenna. That is observable in Figure 6.10 and quantified by a reduction of approximately 4.7 dB (-52.4578 + 57.1661).

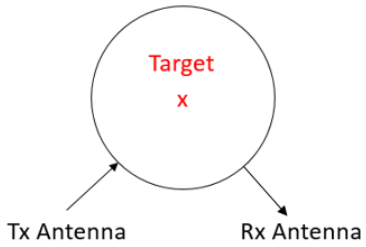

Figure 6.8: Reflection Configuration

Reflection Configuration - Continuous Wave based Software-Defined Radar

Here, the algorithm was changed but the configuration remains the same. Now, we are sending a continuous wave signal. Again, its frequency of operation is chosen in real-time from an available band of values (0.85 GHz - 3.5 GHz). As Figure 6.11 shows, target identification is easily achieved. When target is present, there is a significant decrease in the power that arrives at Rx antenna. In this case, a reduction of circa 5 dB occurs.

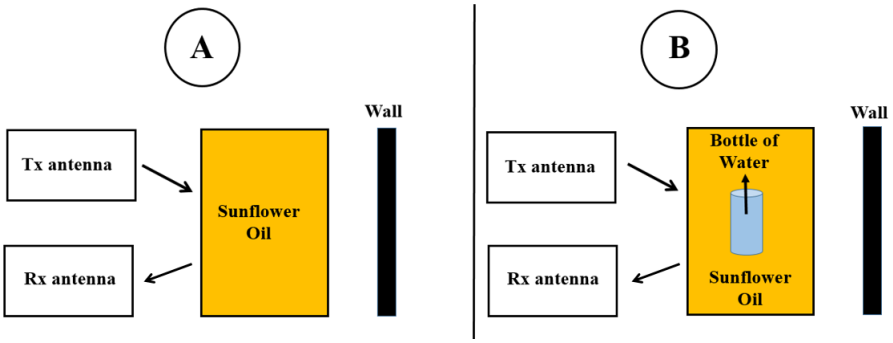

Figure 6.9: Experimental Configuration for Reflection Measurements

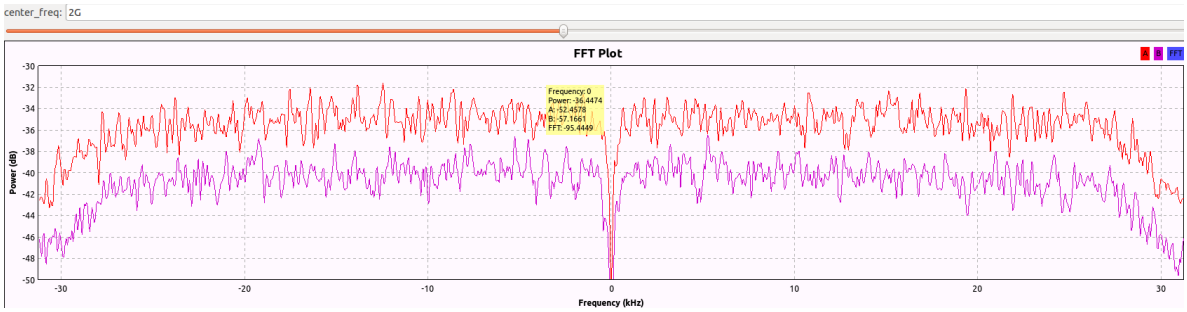

Figure 6.10: Difference between measure with and without target at 2 GHz of center frequency

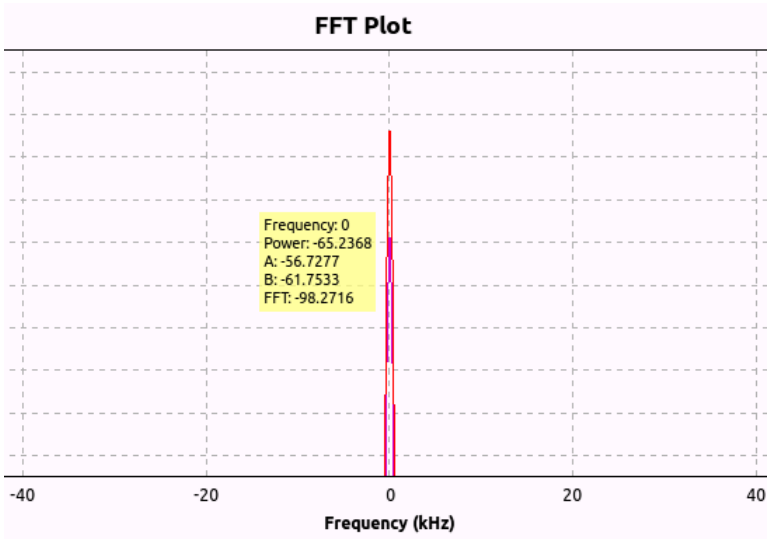

Figure 6.11: Difference between measure with and without target at 2 GHz

Reflection Configuration - Conclusions

After those initial experiments with two different algorithms in a configuration shown in Figure 6.9, we can draw some conclusions. Firstly, both algorithms lead to an identical result. Secondly, as would be expected given the tremendous difference in dielectric constant between water ($\varepsilon_r \approx 77$) and sunflower oil ($\varepsilon_r \approx 3$), there is a clear reduction in received power when target is present. However, that value is less than expected, which is due to a huge loss of information caused by the configuration itself. In other words, the signal coming out from Tx antenna does not arrive totally at Rx antenna but is spread to other locations.

Another problem, well described in the literature review, occurs. The first medium that the signal coming out from the antenna encounters is air. So, when it hits the phantom, one first reflection occurs. The same effect happens in the opposite direction. That causes the received power to be weaker than in ideal conditions.

Transmission Configuration - Introduction

As the previous configuration causes a considerable loss of information, we propose to change to a transmission configuration, which is well described by the previous Figure 6.7. So, here we have one antenna on each side of the phantom.

From now on, we just consider the Continuous-Wave Radar algorithm. However, we will change phantom and dimension of target in order to obtain more information about the resolution of the system.

Transmission Configuration - First Setup

Our first experiment in this new configuration was with sunflower oil as the phantom and bottle of water as the target (Figure 6.12). The resulting power difference between measurement without target and with target was enormous (Figure 6.13). As Figure 6.14 shows, the power difference was of 44 dB at 1.7745 GHz.

Comparing the value obtained in this configuration with the resultant value of the previous configuration, we can conclude that this one gives us an increased resolution. Now, it is possible to differentiate dielectrics with more similar properties than using the former reflection configuration.

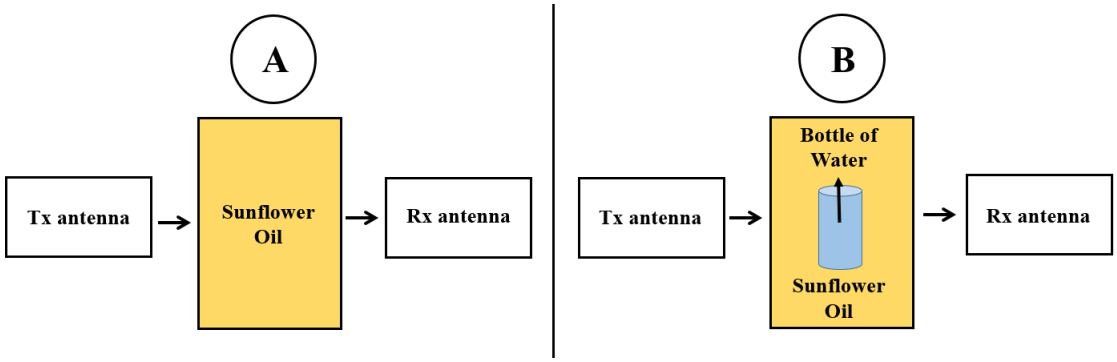

Figure 6.12: Experimental Configuration for Transmission Measurements #1

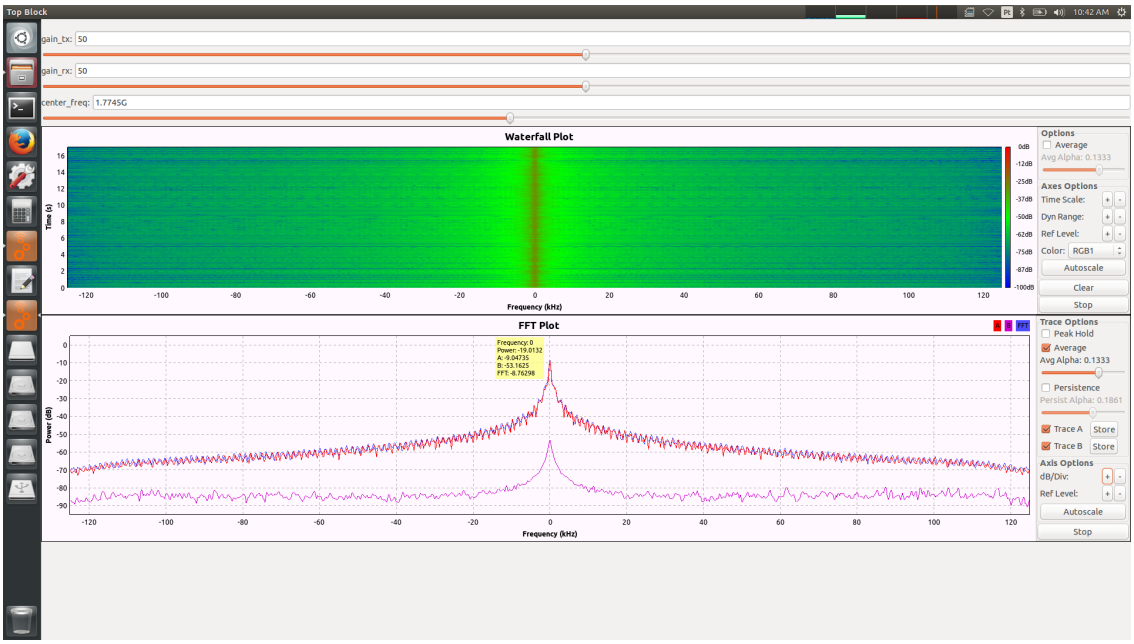

Figure 6.13: Difference between measure with and without target at 1.7745 GHz

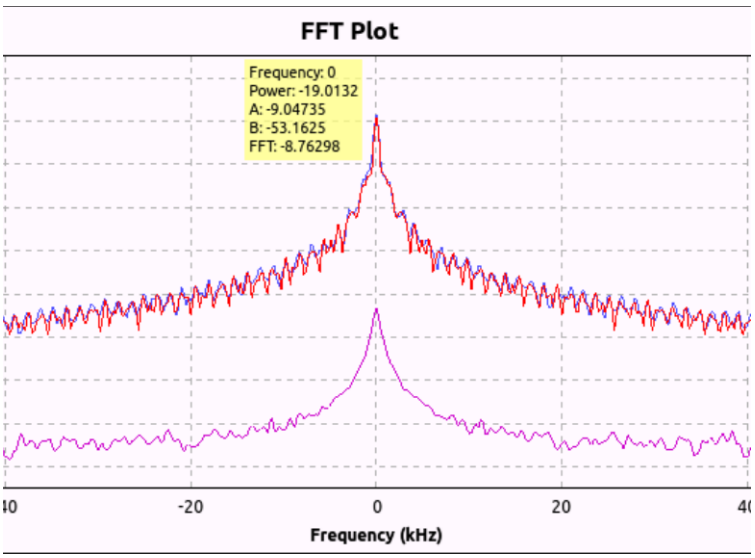

Figure 6.14: Difference between measure with and without target at 1.7745 GHz

Transmission Configuration - Second Setup

After the preceding experiments, we know that it is possible to identify a target inside a phantom when they have dielectric properties quite different from each other. However, that could not be the case. Then, it is interesting to investigate if objects with similar dielectric properties can also be differentiated.

With that goal in mind, we have substituted sunflower oil for juice (Figure 6.15). Although we do not know the precise value of its permittivity/dielectric constant, we can infer that is quite similar to the target (water), as it is constituted by a high percentage of water. Figure 6.16 shows the difference obtained at 1.366 GHz (2 dB). As expected, that difference is not very high but it is still possible to identify the target.

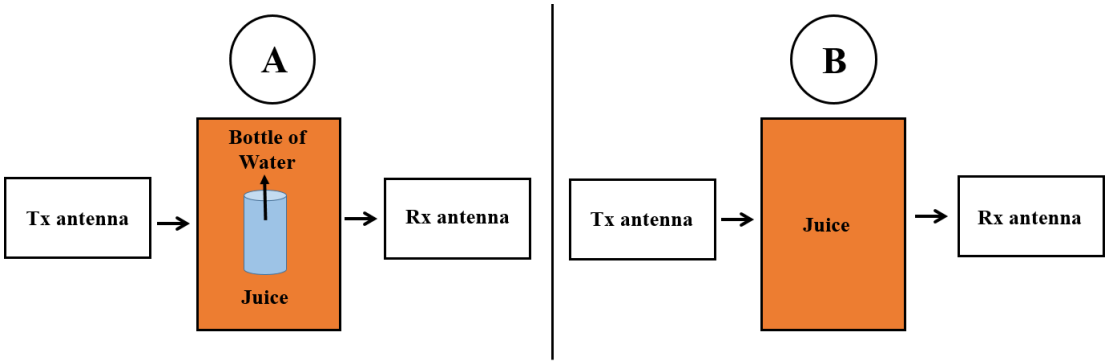

Figure 6.15: Experimental Configuration for Transmission Measurements #2

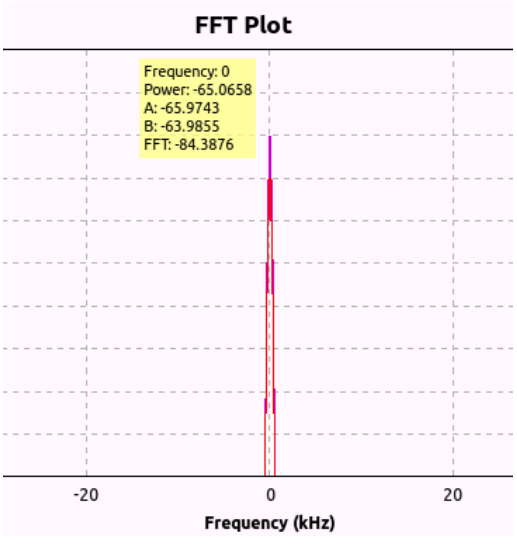

Figure 6.16: Difference between measure with and without target at 1.366 GHz

Transmission Configuration - Third Setup

After testing with a different phantom, we have decided to come back to the first one and to change the dimensions of the target instead.

Changing the small bottle for a syringe of 10 ml full of water (Figure 6.17), we get a smaller target and consequently a smaller difference between measurements with and without it. That is exhibited in Figure 6.18. With this smaller target we just get a difference of 4 dB. However, it is still possible to identify target's presence.

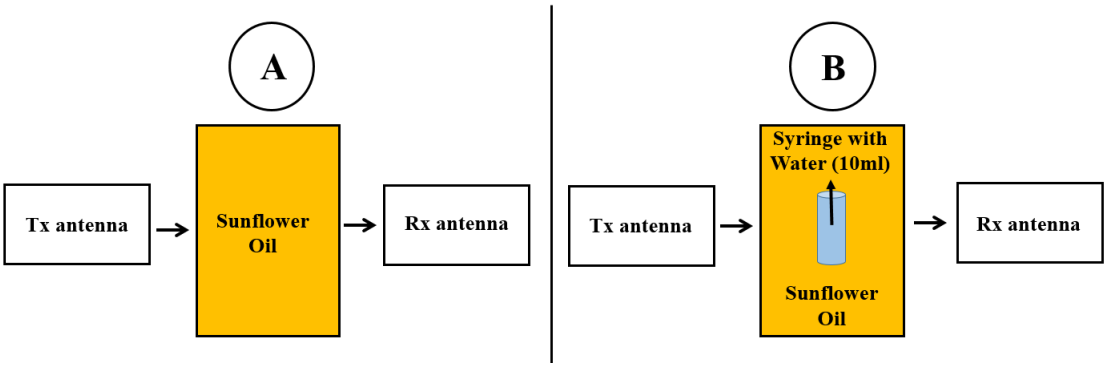

Figure 6.17: Experimental Configuration for Transmission Measurements #3

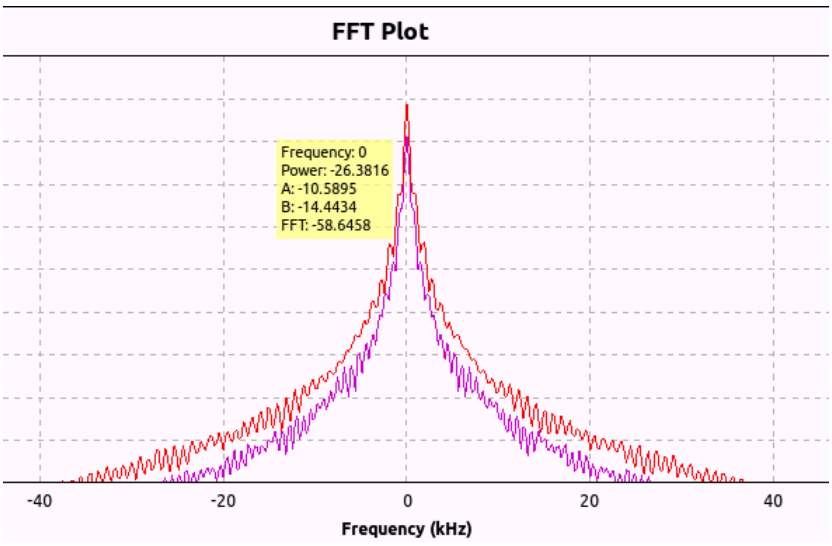

Figure 6.18: Difference between measure with and without target at 1.452 GHz

Transmission Configuration - Fourth Setup

Continuing with oil and water but reducing again the size of the target, changing the 10 ml syringe for a 5 ml one (Figure 6.19), we were not able to detect its presence.

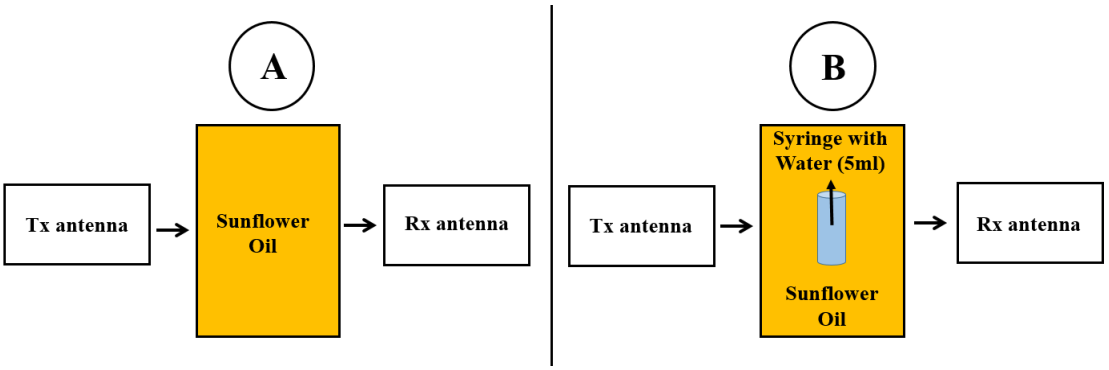

Figure 6.19: Experimental Configuration for Transmission Measurements #4

Transmission Configuration - Fifth Setup

Our last experiment has consisted on testing the resolution limits in the case where the phantom was juice. In this case, even with the bottle of water, the difference obtained was very small. Now, with a 10 ml syringe full of water (Figure 6.20), we were not able to identify any difference.

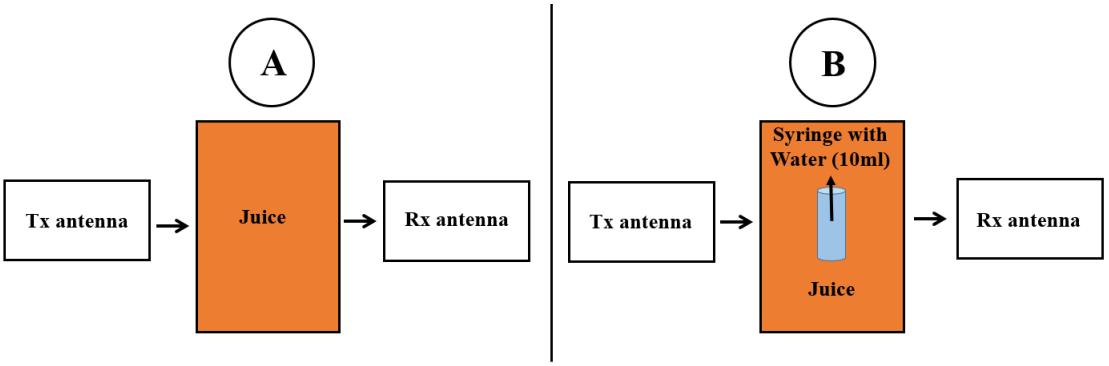

Figure 6.20: Experimental Configuration for Transmission Measurements #5

Transmission Configuration - Conclusions

With this configuration we were able to achieve better results than with the reflection configuration, which is due to the poor performance of that configuration. However, we were still not able to detect the presence of the target in the last two experiments.

6.4 Discussion

This study aimed to evaluate the feasibility of SDRadar as a means to realize Microwave Medical Imaging.

We have used two different configurations. Our reflection configuration had a relatively poor performance, which was due to the considerable loss of information already pointed out. In turn, the transmission configuration had a better performance, allowing us to identify target's presence in many more different scenarios.

Nevertheless, in the last two experiments, we were also not able to detect differences between the cases with and without target. That is mainly due to the resolution of the antennas used in this dissertation, which do not have a very narrow beamwidth and consequently do not have a very high resolution. As Equation 6.4 shows, angular resolution (Δx) depends on the beamwidth (more precisely, half power beamwidth, ψ_{3dB}) and on range.

$$\Delta x = \psi_{3dB} \times R \tag{6.4}$$

In order to increase system's resolution, one can change the type of antennas or implement synthetic aperture.

Furthermore, the gap of air between the antennas and the phantom (which occurs both in reflection configuration as in transmission configuration) also decreases the efficiency of the system. To overcome this problem and following what was referred in Chapter 3, plastic bags filled with a matching liquid can be used.

To sum up, we were able to detect differences between the cases with and without target in three different situations: oil and bottle of water, oil and syringe (10 ml) and juice and bottle of water. Thus, we can conclude that SDRadar is a valid technology for realizing Microwave Medical Imaging.

Chapter 7

Conclusions and Future Work

In this last chapter, a balance of the work performed in this dissertation is made. We explore what was achieved successfully and what can be done in order to improve both developed systems.

7.1 Fulfillment of the Objectives

The first objective of this work was to build a setup, which would be able to monitor vital signs. We have successfully created a system prototype capable of monitoring respiration. It is able to detect interruptions in the normal breathing motion and computes effectively the respiration frequency. Since it works using microwaves, it does not require any sensor attached to the body and consequently does not cause discomfort nor skin irritation. It is thus well suited for traditional applications such as infant observation or emerging applications as the automobile market.

Our final goal was to realize a feasibility study of Microwave Medical Imaging using a Software Defined Radar. Using the same components as to fulfill the first goal, we have demonstrated that this technology allows us to identify objects with different dielectric properties inside a region of interest. The system created is highly flexible, portable and low-cost. Flexibility is given by the SDR hardware platform, GNU Radio and wideband antennas. Furthermore, compared to a VNA, a SDR is much lighter (helping portability) and cheaper (low-cost) and so is the resulting system.

7.2 Conclusions

This dissertation demonstrates that using SDRadar technology it is possible to monitor vital signs and to achieve Microwave Medical Imaging.

As we have seen in the literature review, human bio-sensing includes a wide range of applications. Usually, systems particularly designed for a certain purpose and requiring sensors attached to the body are used. On the other hand, the system that we have created is contactless, highly flexible and adaptable to different RF sensing techniques, being portable and low-cost. Then, it constitutes a very good platform to pursue this area of human sensing by the BRAIN@INESC-TEC group where this dissertation was developed.

In relation to our second system prototype, the fact that we are able to detect materials with different electrical properties inside a phantom makes the system well suited for stroke detection and identification. As stated in Chapter 3, an early and precise diagnostic is of extreme importance in order to increase the number of people receiving thrombolytic treatment. Inasmuch as our system is highly portable and low-cost, it could be available in every Hospital or even inside an ambulance, allowing the covet early diagnosis.

Overall, we feel that this work has shown the disruptive potential of Software Defined Radar technology. Compared to the traditional devices, it introduces many advantageous features such as multipurpose, portability, low-cost and complex processing capabilities.

7.3 Future Work

It can be said that the objectives of this dissertation were successfully completed. However, several improvements can be made. In this section, suggestions for future work will be pointed out, considering each system independently.

SDRadar Human Bio-sensing

- Implementing FMCW (Frequency-Modulated Continuous-Wave) Radar for person localization
- Heart Signal identification based on Machine Learning algorithms (for example, the algorithms referred in Chapter 2)

SDRadar Medical Imaging

- Implementing localization of abnormalities using a rotating platform or more than two antennas (for that purpose, it is mandatory to change hardware platform as well)
- Implementing synthetic aperture or using antennas with narrower beamwidths in order to increase resolution
- Implementing classifiers in order to be able to identify which type of stroke is happening and its severity

References

[1] Compare and contrast mri, ct scan and ultrasound. http://www.cyberphysics.co.uk/topics/medical/compareMRI_CT_US.htm.

[2] What's the difference between an x-ray, ct scan and mri? http://www.northcentralsurgical.com/whats-the-difference-between-an-x-ray-ct-scan-and-mri/.

[3] X-ray. https://en.wikipedia.org/wiki/X-ray.

[4] M. Bassi, M. Caruso, A. Bevilacqua, and A. Neviani. A 65-nm cmos 1.75-15 ghz stepped frequency radar receiver for early diagnosis of breast cancer. *IEEE Journal of Solid-State Circuits*, pages 1741 – 1750, April 2013.

[5] Wikistart - gnu radio. http://gnuradio.org/redmine/projects/gnuradio/wiki.

[6] Usrp b200 (board only) - usrp b200/b210 specification sheet. https://www.ettus.com/product/details/UB200-KIT.

[7] C. Li, V. M. Lubecke, O. Boric-Lubecke, and J. Lin. A review on recent advances in doppler radar sensors for noncontact healthcare monitoring. *IEEE Transactions on Microwave Theory and Techniques*, pages 2046–2060, May 2013.

[8] J. Lin and C. Li. Wireless non-contact detection of heartbeat and respiration using low-power microwave radar sensor. *Asia-Pacific Microwave Conference*, pages 1–4, 2007.

[9] C. Li, J. Cummings, J. Lam, E. Graves, and W. Wu. Radar remote monitoring of vital signs. *IEEE Microwave Magazine*, pages 47–56, 2009.

[10] S. Suzuki, T. Matsui, M. Kagawa, T. Asao, and K. Kotani. An approach to a non-contact vital sign monitoring using dual-frequency microwave radars for eldery care. *J. Biomedical Science and Engineering*, pages 704–711, July 2013.

[11] M. Zakrzewski, A. Kolinummi, and J. Vanhala. Contactless and unobtrusive measurement of heart rate in home environment. *EMBS Annual International Conference*, pages 2060–2063, 2006.

[12] M. Zakrzewski and J. Vanhala. Separating respiration artifact in microwave doppler radar heart monitoring by independent component analysis. *IEEE Sensors Conference*, pages 1368 – 1371, November 2010.

[13] R. Fletcher and S. Kulkarni. Wearable doppler radar with integrated antenna for patient vital sign monitoring. *IEEE Radio and Wireless Symposium, RWW 2010 - Paper Digest*, pages 276–279, January 2010.

[14] A. Vergara, N. Petrochilos, O. Boric-Lubecke, A. Host-Madsen, and V. Lubecke. Blind source separation of human body motion using direct conversion doppler radar. *Microwave Symposium Digest, IEEE MTT-S International*, pages 1321–1324, June 2008.

[15] D. Tan, M. Lesturgie, H. Sun, and Y. Lu. Moving target localization using dual-frequency continuous wave radar for urban sensing applications. *International Radar Conference "Surveillance for a Safer World"*, pages 1–6, October 2009.

[16] M. F. Hilton, R. A. Bates, K. R. Godfrey, M. J. Chappell, and R. M. Cayton. Evaluation of frequency and time-frequency spectral analysis of heart variability as a diagnostic marker of the sleep apnoea syndrome. *Medical and Biological Engineering and Computing*, pages 760–769, 1999.

[17] A. Chapfuwa. Radar signal processing for stand-off life sign monitoring. pages 1–20, 2013.

[18] N. Hafner, I. Mostafanezhad, V. Lubecke, O. Boric-Lubecke, and A. Host-Madsen. Non-contact cardiopulmonary sensing with a baby monitor. *Annual International Conference of the IEEE Engineering in Medicine and Biology - Proceedings*, pages 2300–2302, 2007.

[19] R. Fletcher and J. Han. Low-cost differential front-end for doppler radar vital sign monitoring. *Microwave Symposium Digest, IEEE MTT-S International*, pages 1325 – 1328, June 2009.

[20] A. Droitcour, V. Lubecke, J. Lin, and O. Boric-Lubecke. A microwave radio for doppler radar sensing of vital signs. *Microwave Symposium Digest*, pages 175–178, 2001.

[21] J. Lin. Microwave sensing of physiological movement and volume change: A review. *Bioelectromagnetics*, pages 557–565, 1992.

[22] N. Petrochilos, M. Rezk, A. Host-Madsen, V. Lubecke, and O. Boric-Lubecke. Blind separation of human heartbeat and respiration by the use of a doppler radar remote sensing. *IEEE MTT-S International Microwave Symposium Digest*, pages 175–178, 2001.

[23] Independent component analysis. https://en.wikipedia.org/wiki/Independent_component_analysis.

[24] H. Zhang, S. Li, P. Zhang, Y. Zhang, T. Jiao, G. Lu, and J. Wang. The separation of the heartbeat and respiratory signal of a doppler radar based on the lms adaptive harmonic cancellation algorithm. *Sixth International Symposium on Computational Intelligence and Design*, pages 362–364, October 2013.

[25] A. Kumar, Q. Liang, Z. Li, B. Zhang, and X. Wu. Experimental study of through-wall human being detection using ultra-wideband (uwb) radar. *GC'12 Workshop: Radar and Sonar Networks*, pages 1455–1459, 2012.

[26] L. Solberg, I. Balasingham, S. Hamran, and E. Fosse. A feasibility study on aortic pressure estimation using uwb radar. *IEEE International Conference on Ultra-Wideband*, pages 464–468, September 2009.

[27] A. Fhager and M. Persson. A microwave measurement system for stroke detection. *Antennas and Propagation Conference (LAPC), 2011 Loughborough*, pages 14–15, November 2011.

[28] B. J. Mohammed, A. M. Abbosh, and D. Ireland. Stroke detection based on variations in reflection coefficients of wideband antennas. *Antennas and Propagation Society International Symposium*, pages 2–3, 2012.

[29] A. T. Mobashsher, P.T. Nguyen, and A. Abbosh. Detection and localization of brain strokes in realistic 3-d human head phantom. *IEEE MTT-S International Microwave Workshop Series on RF and Wireless Technologies for Biomedical and Healthcare Applications, IMWS-BIO 2013 - Proceedings*, pages 15–17, 2013.

[30] A. Fhager, T. McKelvey, and M. Persson. Stroke detection using a broadband microwave antenna system. *European Conference on Antennas and Propagation (EuCAP)*, pages 1–3, 2010.

[31] M. A. Khorshidi, T. McKelvey, M. Persson, and H. D. Trefna. Classification of microwave scattering data based on a subspace distance with application to detection of bleeding stroke. *2009 3rd IEEE International Workshop on Computational Advances in Multi-Sensor Adaptive Processing (CAMSAP)*, pages 301–304, December 2009.

[32] M. Persson, A. Fhager, H. Trefna, Y. Yu, T. McKelvey, G. Pegenius, J. Karlsson, and M. Elam. Microwave-based stroke diagnosis making global prehospital thrombolytic treatment possible. *IEEE Transactions on Biomedical Engineering*, pages 2806 – 2817, June 2014.

[33] S. Gabriel, R.W.Lau, and C.Gabriel. *The Dielectric Properties of Biological Tissues: III. Parametric Models for the Dielectric Spectrum of Tissues*. Phys.Med.Biol., 1996.

[34] M. Jalilvand, X. Li, T. Zwick, W. Wiesbeck, and E. Pancera. Hemorrhagic stroke detection via uwb medical imaging. *EuCAP 2011, 5th European Conference on Antennas and Propagation*, pages 2911–2914, 2011.

[35] B. J. Mohammed, A. Abbosh, and D. Ireland. Directive wideband antenna for microwave imaging system for brain stroke detection. *Asia-Pacific Microwave Conference Proceedings, APMC*, pages 640–642, December 2012.

[36] A. Fhager and M. Person. Stroke detection and diagnosis with a microwave helmet. *Proceedings of 6th European Conference on Antennas and Propagation, EuCAP*, pages 1796–1798, March 2012.

[37] A. Zamani, A. Mobashsher, B. J. Mohammed, and A. M. Abbosh. Microwave imaging using frequency domain method for brain stroke detection. *IEEE MTT-S International Microwave Workshop Series on RF and Wireless Technologies for Biomedical and Healthcare Applications (IMWS-Bio)*, pages 6–8, December 2014.

[38] M.Jalilvand, T. Zwick, W. Wiesbeck, and E. Pancera. Uwb synthetic aperture-based radar system for hemorrhagic head-stroke detection. *IEEE National Radar Conference - Proceedings*, pages 956–959, 2011.

[39] H. Peng, Z. Tang, and B. Zong. 2 ghz near-field in-head path-loss model for stroke detection. *IEEE International Conference on Computational Electromagnetics (ICCEM)*, pages 67 – 69, February 2015.

[40] K. Chew, R. Sudirman, N. Seman, and C. Yong. Human brain phantom modeling based on relative permittivity dielectric properties. *International Conference on Biomedical Engineering and Biotechnology*, pages 817 – 820, May 2012.

[41] K. Chew, R. Sudirman, N. Seman, and C. Yong. Human brain phantom modeling: Concentration and temperature effects on relative permittivity. *Advanced Materials Research Vol. 646*, pages 191–196, January 2013.

[42] S. Mustafa, B. J. Mohammed, and A. Abbosh. Novel preprocessing techniques for accurate microwave imaging of human brain. *IEEE Antennas and Wireless Propagation Letters*, pages 460–463, 2013.

[43] J. Marimuthu, A. Abbosh, S. Mustafa, and F. Algashaam. Wideband bandpass filter with wide stopband for microwave imaging system designed for stroke detection. *Proceedings of the 2013 International Conference on Electromagnetics in Advanced Applications, ICEAA 2013*, pages 1314–1316, September 2013.

[44] A. Abbosh and S.Crozier. Strain imaging of the breast by compression microwave imaging. *IEEE Antennas and Wireless Propagation Letters*, pages 1229–1232, January 2011.

[45] X. Li, E. Bond, B. Veen, and S. Hagness. An overview of ultra-wideband microwave imaging via space-time beamforming for early-stage breast-cancer detection. *IEEE Antennas and Propagation Magazine*, pages 19–34, February 2005.

[46] S. A. Rezaeieh, Y.-Q. Tan, A. Abbosh, and M. A. Antoniades. Equivalent circuit model for finding the optimum frequency range for the detection of heart failure using microwave systems. *2013 IEEE International Symposium on Antennas and Propagation and USNC-URSI Radio Science Meeting*, pages 2059–2060, July 2013.

[47] P.C. Pederson, C.C.Johnson, C.H. Durney, and D.G. Bragg. Microwave reflection and transmission measurements for pulmonary diagnosis and monitoring. *IEEE Transactions in Biomedical Engineering*, pages 40–48, January 1978.

[48] S. A. Rezaeieh, K. S. Bialkowski, and A. M. Abbosh. Microwave system for the early stage detection of congestive heart failure. *Special Section on Bio-Compatible Devices and Bio-electromagnetics for Bio-medical Applications*, pages 921–929, September 2014.

[49] Radar. https://en.wikipedia.org/wiki/Radar.

[50] T. Debatty. Software defined radar, a state of the art. *2nd International Workshop on Cognitive Information Processing*, pages 253–257, June 2010.

[51] Lee K. Patton. A gnu radio based software-defined radar. In *Master Thesis*, pages 3–7. Wright State University, 2007.

[52] D. Chinnam, J. Madhusudhan, C. Nandhini, S.N. Prathyusha, Sw. Sowmiya, R. Ramanathan, and K.P. Soman. Implementation of a low cost synthetic aperture radar using software defined radio. *Second International conference on Computing, Communication and Networking Technologies*, pages 1–7, July 2010.

[53] G. Aloi, A. Borgia, S. Constanzo, G. Di Massa, V. Loscrí, E. Natalizio, P. Pace, and F. Spadafora. Software defined radar: synchronization issues and practical implementation. *4th International Conference on Cognitive Radio and Advanced Spectrum Management*, pages 48–52, 2011.

[54] J. Marimuthu, K. S. Bialkowski, and A. M. Abbosh. Stepped frequency continuous wave software defined radar for medical imaging. *2014 IEEE International Symposium on Antennas and Propagation and USNC-URSI Radio Science Meeting*, pages 1909–1910, July 2014.

[55] K.S. Bialkowski, J.Marimuthu, and A.M. Abbosh. Biomedical imaging system using software defined radio. *IEEE International Symposium on Antennas and Propagation USNC/URSI National Radio Science Meeting*, pages 542 – 543, July 2015.

[56] J.Marimuthu, K.S. Bialkowski, and A.M. Abbosh. Software-defined radar for medical imaging. *IEEE Transactions on Microwave Theory and Techniques*, pages 643–652, February 2016.

[57] The big list of rtl-sdr supported software. http://www.rtl-sdr.com/big-list-rtl-sdr-supported-software/.

[58] D. Valerio. Open source software-defined radio: A survey on gnuradio and its applications. Technical report, Forschungszentrum Telekommunication Wien, August 2008.

[59] Roundup of software defined radios. http://www.rtl-sdr.com/roundup-software-defined-radios/.

[60] Hackrf one. https://greatscottgadgets.com/hackrf/.

[61] Nuand - bladerf product brief. http://nuand.com/support.php.

[62] Gnu radio live sdr environment. http://gnuradio.org/redmine/projects/gnuradio/wiki/GNURadioLiveDVD.

[63] Lp0965 antenna. https://www.ettus.com/product/details/LP0965.

[64] Circulator. https://en.wikipedia.org/wiki/Circulator.

[65] Bruhtesfa E. Godana. Human movement characterization in indoor environment using gnu radio based radar. In *Master Thesis*. Delft University of Technology, June 2009.